2018

Decellularized Matrices Effect on the Adaptive Immune Response

Kegan Sowers
Virginia Commonwealth University

Decellularized Matrices Effect on the Adaptive Immune Response

A thesis submitted in partial fulfillment of the requirements for the degree of

Masters of Science at Virginia Commonwealth University

by

Kegan Thomas Sowers

B.S. Engineering Science and Mechanics, Virginia Tech 2016

Advisor: Rene Olivares-Navarrete, D.D.S, Ph.D.

Assistant Professor, Biomedical Engineering

Committee Members: Rebecca Heise Ph.D.
Hu Yang, Ph.D.

Virginia Commonwealth University
Richmond, VA
December, 2018

Acknowledgements

The author wishes to thank his principal investigator Dr. Olivares-Navarrete, as well as Virginia Commonwealth University as an Institution for giving him the support and backing to pursue research. He would also like to thank the love and support of his family as he worked to complete his goals and make the next step in his career.

Table of Contents

List of Figures

Abstract

Decellularized extracellular matrices have been a growing area of interest in the biomedical engineering fields of tissue engineering and regenerative medicine.As these materials move toward clinical applications, the immune response to these materials will be a driving force toward their success in clinical approaches. Fully digested decellularized matrix constructs derived from porcine liver, muscle and lung were created to test the adaptive immune response. Hydrogel characterization ensured that the materials had relatively similar stiffness levels to reduce variability, and *in vitro* studies were conducted. Each individual construct as well as a gelatin control were plated with a co-culture of macrophages and T-cells to measure T-cell proliferation. In addition standard markers of inflammation through qPCR were measured in the macrophage group. Constructs were then placed into animals for 3 and 7 days in addition to a second group that received constructs for 21 days before secondary constructs were placed. These groups were then sacrificed following 3, 7 and 14 days to measure the residual and memory-like response of the constructs. Our results showed that t-cell proliferation was increased with decellularized constructs, particularly in tissue with higher DNA content. *In vivo,* animals with secondary treatments showed extended inflammatory response, driven by Th1 and Th17 polarization suggesting a memory-like response due to recognition of peptides in the constructs from secondary placements.

Chapter 1 – Introduction and Significance

Significant strides have been made in the field of biomaterials and their application to tissue engineering in recent decades. While new materials have proven useful over a range of applications, many researchers are looking back toward the utilization of natural tissue structures and proteins as a method of healing injury and regeneration. Extracellular matrices are comprised of proteins produced by surrounding cells and provide a variety of key functions necessary for the tissues including support, signaling transduction and movement pathways. These proteins form a strict hierarchical structure that can be difficult to replicate *in vitro*, yet are vital to the healthy functions of a normal tissue. Extracellular matrices have become a popular biomaterial source for the development of novel tissue engineering and regenerative medicine approaches to a variety of conditions including cardiac, muscle and skin injuries. To apply these materials to a clinical setting, processes must be used to remove all cells and danger signals that could induce a negative immune response in the affected patient. These processes range in a variety of physical, chemical and enzymatic methods which all can greatly affect the mechanical and chemical properties of the matrix proteins following treatment. Careful process selection is necessary in order to have a final extracellular matrix product for the particular application a researcher or clinician needs. Extracellular matrix can be broken down in a more gentle method in order to maintain the strict protein structure seen in living tissue, or broken down more indiscriminately in order to

develop gels or novel structures while still maintaining similar protein content, albeit in a different structure.

Extracullar matrix constructs consisting of fully broken down proteins have become a popular tool for research methods and potential clinical solutions. Through the utilization of the same protein content found in natural extracellular matrix, gel constructs have become adaptable applications for *in vivo* and *in vitro* studies for tissue engineering approaches. Stem cell research in particular has looked toward decellularized extracellular matrix to influence differentiation of the tissue or cell of choice through direct contact with the naturally occurring proteins and growth factors. These studies have shown promise in the ability of extracellular matrix to influence cells differentiation, and promote growth of specific tissue sets dependent on the extracellular matrix proteins introduced. These methods have even made the step toward clinical applications in areas such as skin regeneration, and future studies show promise to the beneficial capabilities of these matrix proteins.

While *in vitro* and *in vitro* studies have shown promise, the effect of the indiscriminate breaking down of matrix proteins on the immune system has not been fully elucidated. Studies have shown that the extracellular matrix proteins may not have significant inflammatory effects on the innate immune system [1], however extensive research into the effect these protein constructs have on the adaptive immune system has not been a primary focus. The adaptive immune response occurs during and following the initial cleanup, where the innate immune system collects these degraded proteins and presents them to the adaptive immune system as a way to develop antibodies. Antibody production introduces further inflammation, and is the building blocks to the memory-like

system the body can deploy. With the small peptides and proteins from the extracellular matrix being collected in the high-inflammatory environment of injury sites, the adaptive immune system could collect these naturally found proteins and develop antibodies against them. This is generally the method that auto-immune diseases attack native tissue, usually due to a genetic defect in the protein. When the immune system recognizes these native proteins or peptides and antibodies for them are produced, increased inflammation at these proteins could occur. Further studies into the adaptive immune response to fully deconstructed decellularized extracellular matrices are needed to elucidate the interaction of the immune system with these broken down proteins.

Chapter 2 – Specific Aims

The specific aims of this project are to elucidate the interaction between fully digested decellularized extracellular matrix constructs and the adaptive immune response. The aims are split into an *in vitro* and *in vivo* aim respectively.

1.) *In vitro -* *The objectives of the in vitro aim are to characterize the decellularized matrices to be used in the study and determine the immune response in vitro.* Differences in each of our target tissue of interest may create differences in immune response. *We hypothesize that digested decellularized matrices will influence macrophage and T cell activation.*

2.) *In vivo-* *The objectives of the in vivo aim are to characterize the decellularized matrices to be used in the study and determine the immune response in vitro.* Differences in each of our target tissue of interest may create differences in immune response. *We hypothesize that digested decellularized matrices will influence macrophage and T cell activation.*

Chapter 3 - Background

3.1 Biomaterials

As medical and scientific advances continue, novel materials are being utilized to treat new problems or challenges in human health. The use of materials in treating human condition has been widely applied for centuries but with a greater understanding of mechanisms of disease and injury, new materials are being applied in hopes to find cures or methods of regeneration for these diseases. Biomaterials can range across a wide variety of materials, from metals and ceramics to polymers dependent on the needs of the affliction [2]. For example, in dental and bone applications metals or ceramics fulfill the necessary mechanical properties while eliciting a relatively low immune response [3]. In the case of organ damage or failure, novel replacement materials must be able to fulfill multiple criteria including function while maintaining a low toxicity to reduce the immune response. These biomaterials can be utilized for a range of functions including tissue regeneration, drug release or functional tissue replacement. The success of these biomaterials is dependent on the ability to succeed in its primary function. In the case of bone and dental implants, the material must be able to undergo continuous stress while maintaining the integration at the site of implementation without failure [4], [5]. For drug delivery hydrogels, the biomaterial must be able to maintain its structure such that the delivery molecules can be released over an extended time at a set rate [6]. In the case of organ failure and replacement, novel

materials are being studied in hopes of developing a method for increasing the function in a diseased state, or even potential regeneration of the tissue of interest.

While success of a biomaterial is primarily dependent on the ability to function, many factors can lead to the failure of the implant. Failure of an implant can lead to subsequent apoptosis of surrounding tissue, as well as buildup of fibrotic tissue and a limitation on organ function [7]. To prevent implant failure, the material must be able to maintain a microenvironment conducive to tissue function, including maintenance of immune system balance. In the case of organ transplantation, the host must be immune-compromised to reduce the risk of Graft-versus-Host Disease (GvHD). In the case of GvHD, the host immune system may recognize the transplanted tissue as genetically dissimilar, leading to subsequent attack by the host immune system [8]. This in turn leads to tissue apoptosis and an influx of pro-inflammatory factors that are not conducive to tissue function or survival.

One biomaterial that is gaining interest as a treatment option is the utilization of decellularized matrix tissue to mimic the organ of interest as well as facilitate the regrowth of tissue [9], [10]. Current treatments being used in a clinical setting primarily include autologous bone matrix, acellular skin treatments for burn victims and acellular heart valve procedures known as the Ross procedure [11]–[13]. With the major reduction in cells, the risk of host immunity recognizing the tissue as foreign is reduced. While the decellularized matrix alone is not capable of functioning as the replacement tissue there is hope that the scaffold of the tissue containing the similar extracellular components to its target treatment could lead to cell infiltration and regrowth. Due to their high variability in source, as well as the ability to utilize decellularized tissues of

interest as a treatment option, decellularized matrices have become a biomaterial of choice in current biomedical research.

3.2 Decellularized Extracellular Matrices

Decellularized matrix and matrix components are becoming increasingly popular tools in research and clinical settings for numerous applications. The properties of the decellularized matrix is primarily dependent on the components of the extracellular matrix of the tissue of origin. In the case of skin, the primary proteins are collagen type I and elastin, which provide the tissue with the mechanical properties to stretch and undergo large deformation. Cartilage however is primarily proteoglycan and collagen type I and II to allow it to provide the dampening capabilities for joints. The decellularized matrices of each of these tissues would therefor provide differing mechanical properties and functions for their respective treatments.

There are physical and chemical processes that effect the composition of the decellularized matrices following processing. The most common physical treatment methods to remove cellular components include rapid temperature change through freezing and electrical disruption. Rapid freezing leads to microcrystal formation in the cell membrane, leading to effective lysing of the cell. One other aspect of the freezing is that larger crystals can form, which can alter the conformation of the extracellular proteins allowing for changes in porosity to occur. Applied electrical pulses can disrupt the channels in the cell membrane causing an ion unbalance and subsequent cell apoptosis.

Chemical processes include washes of the tissue with ionic or non-ionic detergents. Ionic detergents such as sodium dodecyl sulfate (SDS) efficiently lyse cells and allow for soluble intracellular components to be rinsed away. Subsequent washes with acids and endonucleases break down nucleic acids and solubilize them to be removed with further washing. Non-ionic detergents such as Triton X-100 effectively disrupt the lipid-lipid interactions in cell membranes, leading to effective lysing and cell apoptosis. While these treatments are effective at cellular removal, they can disrupt the protein structure [14]. SDS in particular has shown to bind and remove glycosaminoglycans (GAGs) and other proteoglycan structures [15]. This can effectively change the protein composition of the extracellular matrix in comparison to the native tissue, especially in tissues with high levels of GAGs such as cartilage or skin.

Enzymatic treatments can also effectively decellularize tissues. In particular endonucleases are extremely effective at breaking down genetic content following cell lysing. Trypsin has also shown to be an effective enzymatic treatment for cell removal [16]. Due to the protein-cutting nature of enzymes, many enzymes can affect the protein structure of the remaining extracellular matrix. In treatments or studies that do not require intact protein structures, enzymes can provide efficient decellularization. In addition, collagenase and pepsin are enzymes that breakdown the extracellular matrix entirely, ensuring removal of cells from the entirety of tissues as well as tunable breakdown of protein structures [17].

Due to the wide variety of applications specified decellularization processes can be utilized to ensure the post-treatment matrices contains the necessary parameters.

3.3 Innate Immune Response

Immune response to these biomaterials can range across a spectrum dependent on the innate immune response reaction. The initial response to any sort of implanted biomaterial can dictate the subsequent immunological reaction, which can drive healing, fibrosis or tissue death [18]. These “first responders” include tissue-resident macrophages, neutrophils natural-killer cells and dendritic cells. Phagocytic macrophages and dendritic cells phagocytize pathogens or danger signals in the area and influence the rest of the immune system with signaling [19]. Danger signals include nuclear or cytosolic proteins that can be produced by damaged tissues and cells that do not undergo the standard apoptosis methods. Macrophages and dendritic cells phagocytize these biomolecules and can undergo a phenotype change toward a pro-inflammatory response, producing cytokines such as TNFα, IL-1B and IL-6 that exacerbate the immune response [19]. Generally, activated macrophage phenotype is characterized by a pro-inflammatory response (M1), anti-inflammatory (M2) or naïve (MΦ) phenotype [20]. Pro-inflammatory macrophages are generally activated by pathogens, however in the presence of Danger Signal Molecules similar pro-inflammatory responses can occur. Upon activation, macrophages can communicate with other innate and adaptive immune cells through cytokine production, microenvironment conditioning as well as antigen-presentation. Pro-inflammatory activation leads to interleukin (IL) release which further recruits immune cells to the area prolonging the inflammatory response. Anti-inflammatory activation leads to production of cytokines which help control the immune response while also recruiting stem cells to promote healing. While convention dictates these states as the primary phenotypes of

macrophage activation, in reality the response is more along a gradient where immune cells may not fall directly into one of the phenotypes.

Decellularized extracellular matrices can induce a response from the innate immune system that ranges from inflammatory to anti-inflammatory [21], [22]. Studies have shown differences in response dependent on the matrix purity, protein structure as well as mechanical properties. While the decellularized process removes the majority of cellular and genetic components, there can still be residual material which can lead to danger signaling in the innate immune system [23]. Recognition of these signals through Toll-like receptors (TLR) can lead to a signaling cascade producing a pro-inflammatory response and the presentation of antigens. In addition to RNA and DNA, proteins and free cytokines can induce the same danger signal pathway in the innate immunity.

3.4 Adaptive Immune Response

In addition to stimulatory factor production, macrophages and dendritic cells also act as antigen presenting cells (APCs). Antigen presentation is one of the primary forms of communication between the innate and adaptive immune response. The adaptive immune system is comprised of cells from the lymphocytic lineage, T cells and B cells. These cells can bind to the presented antigens leading to activation. Depending on the type of antigen, different T cell activations can occur. Major-histocompatibility complex type I (MHC I) antigens generally are presented by APCs to denote whether the cell is foreign versus self. This can lead to an activation of CD8+ cytotoxic T cells, which attack foreign bodies and virus infected cells [24]. Major-histocompatibility complex type II (MHC II) antigens lead to activation of immunomodulatory CD4+ T helper cells. These

cells produce a variety of inflammatory and anti-inflammatory factors that can either prolong inflammatory response or attenuate it. T helper cells are commonly divided into four subsets, though continuing studies are showing there may be a more robust phenotypic layout [25], [26]. The four most prevalent subsets include type 1 helper cells (Th1), type 2 helper cells (Th2), type 17 helper cells (Th17) and T regulatory cells (Treg). Th1 cells produce interferon gamma (IFN-γ), a cytokine that promotes inflammation through activation of other innate and adaptive immune cells [27]. Typically released in bacterial or viral infection, IFN-γ activates macrophages toward the M1 phenotype increasing phagocytic activity and increasing CD4+ T cell activation through a positive feedback loop [28]. Th2 cells secrete anti-inflammatory factors IL-4 and IL-13, which reduce macrophage activation and promote a more naïve lymphocytic phenotype [29]. Th17 cells release stimulatory interleukin 17 (IL-17), as well as other stimulatory cytokines including IL-21 and IL-22 [30]. IL-17 has been shown to be a regulator of the pathogenesis of numerous auto-immune disorders as well as effective stimulators of B-cell and T-effector memory cells [31]. Tregs are known as being modulators of inflammation by releasing IL-10, which has shown to reduce inflammatory phenotype in the innate immune cells [32].

B cells are the primary cells associated with the humoral immunity. B cell receptors bind to antigens, which they can then internalize through endocytosis before producing an MHC II antigen to present to T cells. Upon activation, CD4+ T helper cells then produce a positive feedback loop through stimulatory cytokine production leading to the rapid proliferation of these B cells. These B cells can activate become plasma cells which begin producing antibodies for this specific antigen allowing for natural killer

cells and macrophages to bind and phagocytize [33]. In addition, some of the B cells may stay dormant, producing the effective “memory” to the antigen to be activated again when encountered [34]. While typically thought of as primarily pathogen specific, B cells can produce antibodies for tissue specific proteins and peptides as well as potentially danger signals. These reactions form the basis for the pathogenesis of some autoimmune disorders [34], in which tissue-specific antigens are taken by the immune system, and antibodies for these antigens are produced leading to the attack of native tissue by the immune system.

Chapter 4 – Aim 1

Biomaterial Characterization and *In Vitro* Immune Response

Introduction

Decellularized matrices undergo many different processes to form the finalized material to be utilized in research or clinically. The different process can alter the physical and chemical composition of the decellularized matrix. While we focus on the utilization of digested gels, the overall mechanical properties can be adjusted with a backbone structure, in our case Methacrylated Gelatin (GelMA). Differences in stiffness can influence the immune response, as can the presence of danger signals. To determine the effectiveness of the decellularization process, DNA quantification can measure the relative DNA levels before and after the decellularization process. *The objectives of this aim are to characterize the decellularized matrices to be used in the study and determine the immune response in vitro.* Differences in each of our target tissue of interest may create differences in immune response. *We hypothesize that digested decellularized matrices will influence macrophage and T cell activation.*

Materials and Methods

Extracellular matrix processing

Extracellular matrices were prepared using a modified method of Reing et al. [35], altering only two wash durations. Briefly, liver, lung and muscle pieces from a porcine animal model were transferred into Erlenmeyer flasks and underwent a series of chemical and enzymatic washes on an orbital shaker at 250 rpm. These consisted of three 2-h washes with 0.25% trypsin EDTA to provide thorough washing; three 15-min washes in deionized (DI) water; and one 15-h wash in 70% ethanol. This was followed by one 15-min wash in 3% hydrogen peroxide in DI water; two 15-min washes in DI water; and one 6-h wash in 1% Triton X-100 in EDTA/Trizma; and one 15-h wash in fresh 1% Triton X– 100 in EDTA/Trizma. The cartilage matrices were then washed three times for 15-min in DI water, followed by a 2-h wash in 0.1% peracetic acid (PAA)/4% ethanol, two 15-min washes in phosphate buffered saline (PBS), and two 15-min washes in DI water. Resulting pieces were frozen at 20 C for subsequent lyophilization before utilization in *in vitro* and *in vivo* testing.

GelMA synthesis

The detailed experimental procedure has been described previously [36]. In short, type A gelatin derived from porcine skin tissue was dissolved in calcium and magnesium free phosphate buffer solution, and the pH was adjusted with 5 M sodium hydroxide or 6 M hydrochloric acid. Subsequently, MAA (94%) was added dropwise to the gelatin solution under magnetic stirring at 500 rpm while maintaining 60° C. The

reaction proceeded for 3 h, and then the pH was readjusted to 7.4 to stop the reaction by quenching with phosphate buffer solution. After being filtered, dialyzed for 7 days in RO water, and lyophilized, the samples were stored at −20 °C until further use.

Formation of ECM gels

Therefore, ECM hydrogels were created using a modified version of the method of Freytes et al. [37]. Processed lung, liver and muscle fragments (approximately 2 mm x 2 mm) were frozen at 20 C overnight before lyophilization for 24 h. Lyophilized tissue was digested with 30 mg/mL pepsin in 0.01 N HCl for 48 h at RT to make ECM digests at a concentration of 10 mg (dry weight) per mL solution. ECM digest was stored at 20 C until gels were created. ECM digests were adjusted to physiological pH in PBS with 0.01 N NaOH, to form matrix gels with a final concentration of 6 mg (dry weight)/mL. 5% GelMA was added to the ECM gels to aid in gelation and to maintain an approximately equivalent stiffness level between all the groups. ECM/GelMA solutions were sterilized under UV light for approximately three hours before continuing the experiment. 0.05% LAP photoinitiator was added to the ECM gels. The matrix gels (500 µL) were then coated on 24-well plates or prepared for surgery in syringes. ECM digests were allowed to gel for 5 minutes under 405 nm Blue Light. Cartilage matrix gels were then hydrated with 500 µL Mg2+ and Ca2+-free PBS (Life Technologies, Carlsbad, CA, USA) for 1 h. PBS was then aspirated before cell culture experiments began.

Hydrogel Rheology

One milliliter of pre-polymer ECM pre-gel and GelMA solution mixed with .05% weight/volume Lithium Phenyl(2,4,6-trimethylbenzoyl) phosphinate (TCI America) was pipetted into a two centimeter mold. Samples were then exposed to 9.6 mW/cm2 Blue light 405 nm for 180 seconds. Samples were then removed from the petri dish and tested using a TA Instruments Discovery HR-3 model rheometer. Samples were tested under conditions of an amplitude sweep from .01 to 10% strain at a frequency of 1 rad/s. In addition, a frequency sweep from .1 to 10 rad/s was conducted at a constant strain of .05%. All tests were conducted at 37°C to best represent physiological temperature.

Cell Isolation and culture

Primary macrophages were isolated from femurs of 8-12 week-old female C57BL/6 mice (The Jackson Laboratory, Bar Harbor, ME) under VCU IACUC approval based on previously established protocols. Briefly, bone marrow cells were flushed from the femurs using Dulbecco's phosphate-buffered saline (Life Technologies, Carlsbad, CA). Red blood cells were removed from flushed bone marrow by addition of ACK Lysing Buffer (Quality Biological, Inc., Gaithersburg, MD). Cells were counted (TC20™ Automated Cell Counter, Bio-Rad Laboratories, Hercules, CA) and plated in a 175 cm2 flask at a density of 500,000 cells/mL in 30mL RPMI 1640 media (Life Technologies) supplemented with 10% fetal bovine serum (Life Technologies), 50U/mL penicillin-50 µg/mL streptomycin (Life Technologies), and 30ng/mL macrophage colony-stimulating factor (M-CSF, PeproTech, Rocky Hill, NJ). Cells were cultured at 37°C, 5% CO2, and 100% humidity. Fresh media supplemented with M-CSF was added after four days. After seven days of exposure to growth factors, macrophages were passaged with

Accutase (Life Technologies) at room temperature for 1 hour and seeded onto ECM hydrogel coated plates for experimentation.

Primary T cells were isolated from spleens removed from the same 8 week-old female C57Bl/6 mice. Naïve CD4+ T cells were then separated by negative selection using isolation columns (Milteny Biotec, San Diego CA). Briefly, spleens were crushed between two sterilized microscope slides to release cells, and red blood cells were lysed (ACK Lysing Buffer, Quality Biological, Inc.). A single cell suspension was magnetically labeled using a cocktail of biotinylated monoclonal antibodies and anti-biotin microbeads labeling agents to deplete non-CD4+ splenocytes. Untouched isolated CD4+ T cells were then cultured in complete RPMI 1640 containing 10% FBS, 1% L-Glutamine, 1% penicillin-streptomycin, and 0.1% 2-mercaptoethanol and activated for 48 hours in plates pre-coated with 5μg/mL anti-CD3e mAb (Biolegend) and treated by 2μg/mL anti-CD28 to promote proliferation before being used in experiments.

In vitro Macrophage Activation

To compare macrophage activation on the different Ti surfaces, secreted factors were quantified following 24 hours of culture. Differentiated macrophages were plated on Hydrogel coated well plates at a density of 50,000 cells/cm^2. Media was removed and levels of pro- (IL1β, IL6, and TNFα) and anti- (IL4 and IL10) inflammatory markers for macrophage activation were measured by enzyme-linked immunosorbent assay (ELISA) based on manufacturer's protocol and normalized to cell number. Cell number at was determined using DNA quantification assay and a standard curve plated with a known protein quantity plated in serial dilution. DNA levels were quantified in cell lysates using the Quant-iT™ PicoGreen dsDNA Assay Kit (Invitrogen, Life Technologies) as per

manufacturer protocol. RNA was isolated from plated macrophages with TRIzol (Life Technologies) following manufacturer's instructions. Equal amounts (1000 ng) of RNA were reverse transcribed into cDNA for each sample (High Capacity cDNA Kit, Life Technologies). The resulting cDNA was used in real-time quantitative polymerase chain reaction (qPCR) reactions using Sso Universal Probes Supermix (Bio-Rad, Hercules, California) to measure mRNA quantities of pro and anti-inflammatory factors.

In Vitro Co-Culture Model

Interactions between T-cells and macrophages were examined using direct co-culture experiments. In indirect co-culture experiments, macrophages were cultured on Ti surfaces for 24 hours at a density of 50,000 cells/well and media with secreted factors (conditioned media) were then collected and used to treat activated T-cells in a separate 24 well plate. For direct culture experiments, macrophages were grown on decellularized matrix hydrogels for 24 hours and then activated T-cells were added to the culture in a 1:1 ratio. These cells were allowed to interact for an additional 24 hours before media, and non-adherent T-cells were collected for analysis. To assess proliferation, CD4+ T-cells were treated with carboxyfluorescein succinimidyl ester (Yellow, Molecular Probes, ThermoFisher) during the direct co-culture with macrophages. Activated T-cells cultured with CD3 and CD28 (+) and unactivated T-cells cultured with only CD3 on GelMA were used as control groups. After 24 hours of interaction, cells were collected and analyzed by flow cytometry. Changes in CD4+ T-helper proliferation were determined by flow cytometry using a CellTrace Yellow Cell Proliferation Kit (ThermoFisher Scientific, Waltham, MA). Stained cell suspensions were analyzed using the Guava® easyCyte 6-2L Benchtop Flow Cytometer (MilliporeSigma)

instrument with a total of 10,000 events were measured with three replicates for each measurement. Results were analyzed using guava Soft 3.1.1 InCyte software.

Statistical Analysis

A one-factor, equal-variance analysis of variance (ANOVA) was used totest the null hypothesis that the group means are equal, against an alternative hypothesis that at least two of the group means are different, at the $\alpha=0.05$ significance level. Upon determination of a p-value less than 0.05 from the overall ANOVA model, multiple comparisons between the group means were made using the Tukey-HSD method. All statistical analysis was completed using GraphPad V5 software.

Results and Discussion

Gel Rheology

Gel Rheometry conducted on the gel constructs was to ensure that the stiffnesses of the matrices were consistent such that there was not a strong difference. Differences in stiffness between matrix substrates have shown the ability to influence macrophage activation, fibrosis and healing [38]. Rheometry results across a frequency and amplitude sweep showed no significant differences between the GelMA group and hydrogel constructs. All storage modulus values fell between 200 and 300 Pascals (Figure 1), which is representative of extremely soft tissue such as brain tissue [39]. While precautions and testing can be conducted to ensure comparable mechanical properties, even slight differences have been shown to influence macrophage activation [40]. The stiffness provided allows for injection in *in vivo* studies, while maintaining its structure over time without risky solubilizing.

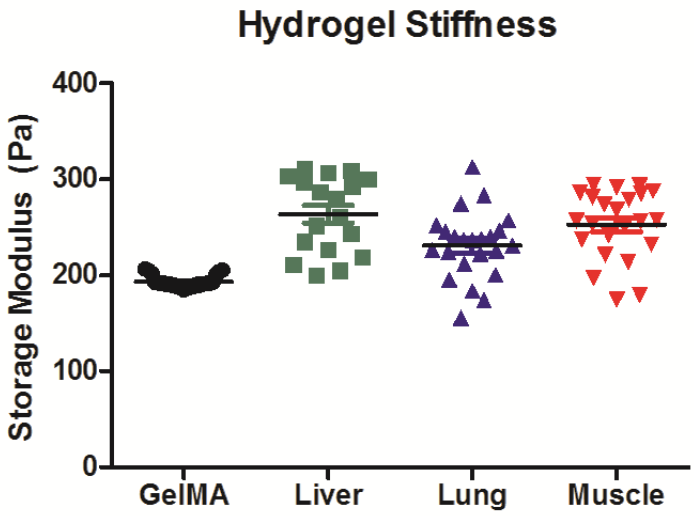

Figure 1: Storage modulus values for each decellularized matrices treatment. 20 mm diameter pucks, 1 mL in volume of gel solution was used for each rheometry puck.

DNA Quantification

To measure purity of the processed samples following treatment, DNA quantification was conducted before and after processing to quantify DNA removal in comparison to dry weight. Prior to decellularization, liver contained 70.415 ng/mg dry weight DNA, 26.243 ng/mg dry weight DNA in lung tissue and 8.0738 ng/mg dry weight DNA in muscle tissue. Following the decellularization process, 97-98% of all DNA content was removed from the tissue as shown in Table 1. These values are representative to those values found in literature and commercially [41], indicating that while the prevalence of Danger Signals is still a concern, it does fall within the approved range of acceptable values in research and industry. Microscopic image of pre-treatment versus post-treatment shown in (Figure 3).

	DNA pre-processing (ng/mg dry weight)	DNA post-processing (ng/mg dry weight)	Total Percentage Reduction
Liver	70.415	1.7061	97.58
Lung	26.243	0.4038	98.46
Muscle	8.0738	0.1152	98.57

Table 1: DNA content prior to and following the decellularization processing.

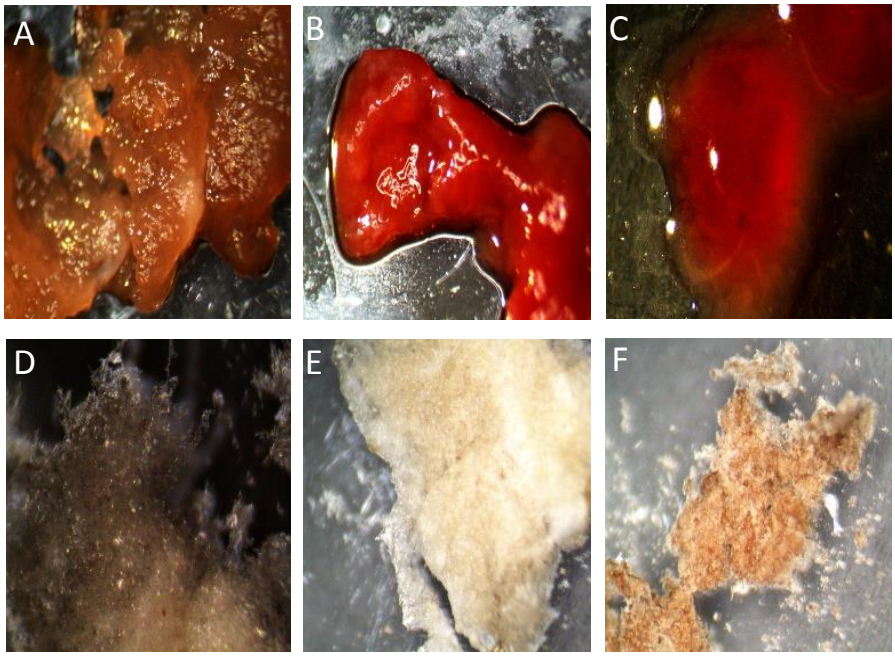

Figure 2: Microscopic imaging of Muscle, Lung and Liver pre-processing (A,B,C) and post-processing (D,E,F) respectively.

Macrophage Activations

Following 24 hours of culture, expression of both pro and anti-inflammatory markers were measured by qPCR. No statistically significant changes in mRNA expression of pro-inflammatory markers Il-6, Tnfα or Il-1β between the liver, lung and muscle groups compared to the control (Figure 3). In addition, no statistical differences were seen in the comparisons of the treatment groups. Similarly, no statistically significant changes in marker of anti-inflammatory Il-10 were seen. While on the surface

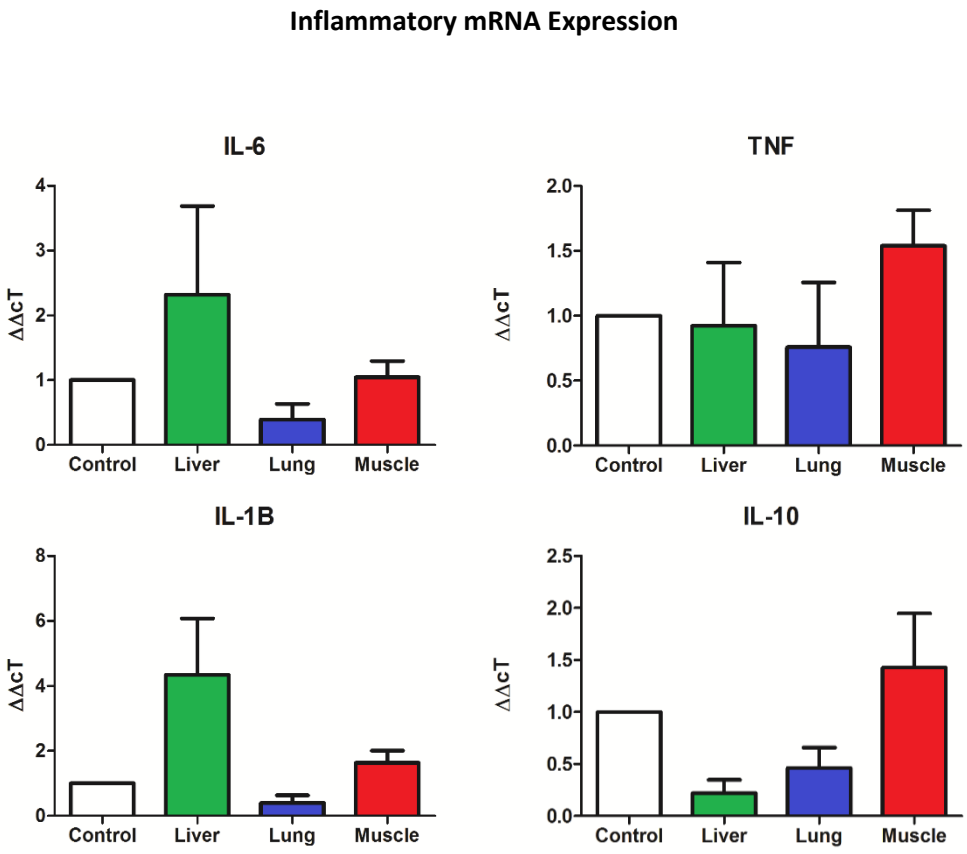

Figure 3: Changes in mRNA expression in primary macrophages plated on protein coated well plates (n=3). # p<0.05 vs control, @ vs Liver coating, & vs Lung coating.

these results may be surprising, many studies have shown that while danger signals and exogenous peptides from decellularization processing can cause inflammation, others have publicized immunomodulatory behavior by decellularized matrices [22], [42]. Following proper decellularization procedure, and reducing residual DNA content to a minimum, immune response can be reduced. Another potential explanation for the reduced immune response relies on the later time point (24 hours) of termination of cell culture experimentation. By 24 hours, macrophages may already be producing the pro or anti-inflammatory cytokines, and expression of these markers may have been reduced to closer to standard levels.

Macrophage protein secretion drives further immune response by activation and recruitment following activation in response to exogenous peptides or danger signals. Significant differences in inflammatory cytokine production were seen following 24 hours of macrophage culture on each of the decellularized matrix protein coated well plates compared to control (Figure 4). Liver and muscle treatment groups showed the greatest increase in pro-inflammatory cytokine TNFα production in comparison to the control. Pro-inflammatory cytokine IL-6 was increased in all treatment groups, while IL-1β secretion showed no statistical differences between the groups and the control. Anti-inflammatory cytokines IL-4 and IL-10 secretion was increased significantly in all treatment groups, with exception to IL-10 for the liver treatment with respect to the control. Overall, each of the treatment groups did have an affect on the initial cytokine secretion following direct plating on the decellularized matrices. Xenograft antigenicity can affect the murine immune system through recognition of certain peptide configurations as non-self or foreign material. In addition, residual DNA would increase this immune system activation, in comparison to an allograft or autograft where recognition of self would be more likely to occur.

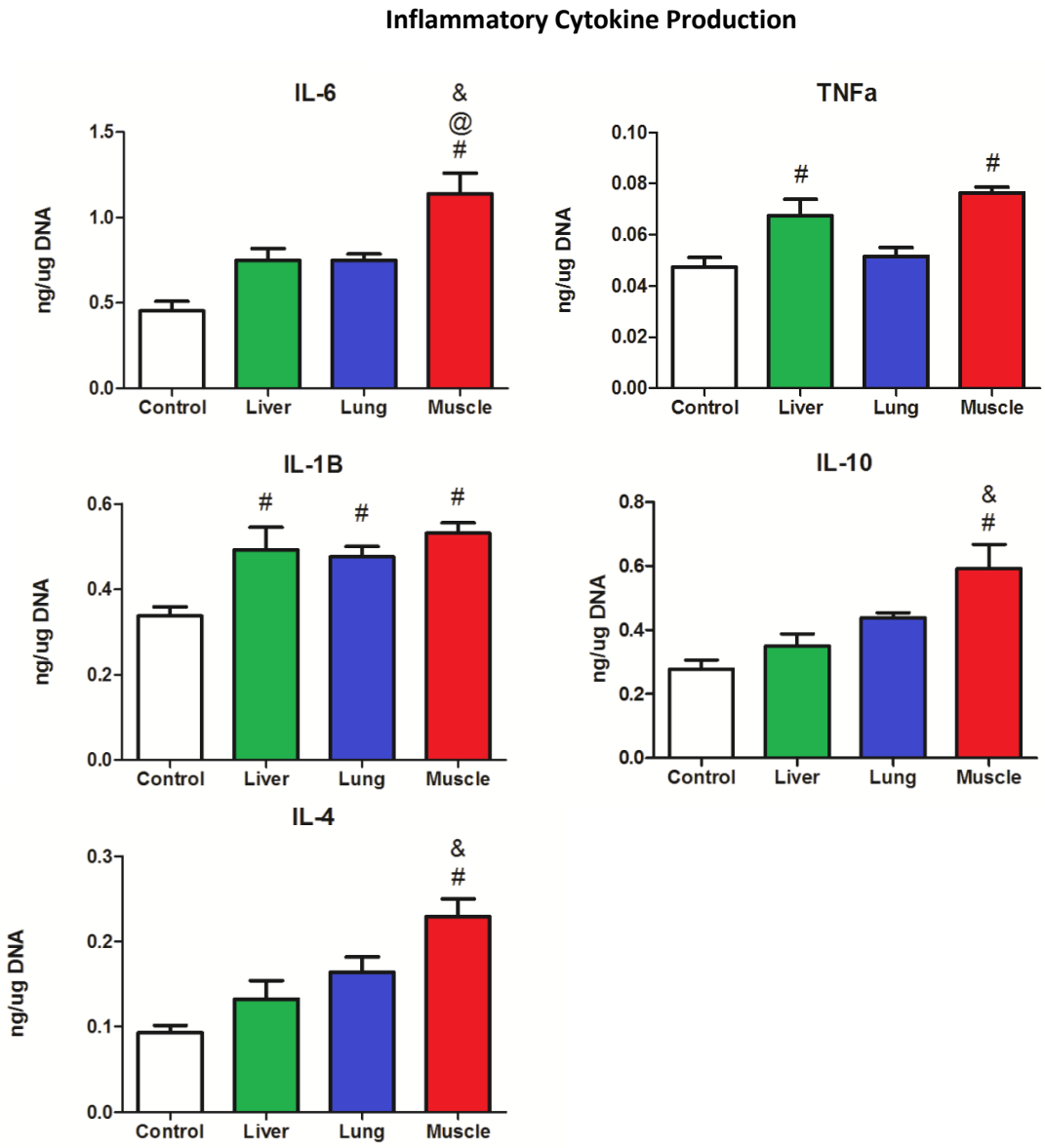

Figure 4: Changes in cytokine production from macrophages plated on ECM constructs (n=6). # p<0.05 vs control, @ vs. Liver treatment, & vs. Lung treatment.

T cell activation

To determine the incidence of antigen presentation by macrophages, macrophages and CD4+ T helper cells were co-cultured directly. Following 24 hours of macrophage culture on each of the hydrogel coated plates, T cells were plated at a 1:1

ratio and allowed 48 hours for proliferation. Direct interaction between the macrophages and the T-cells on all treatment groups led to the ability to proliferate. Liver and muscle groups showed the highest incidence of T cell proliferation (CFSE low) of the treatment groups (Not Shown). GelMA and lung treatment T cells both showed the ability to proliferate, but the groups with higher inflammatory profiles produced greater rates of proliferation. This indicates that the decellularized matrix constructs are inducing macrophage presentation of Major Histocompatibility Class II antigens capable of activating CD4+ T helper cells which drive further adaptive immune response.

Conclusion

Decellularized matrices are becoming a common tool for biomedical research and clinical applications. Due to their variability in structure and function, decellularized matrices of a multitude of tissue origins are being utilized to treat a variety of ailments. When decellularizing a matrix, care must be taken in choosing the best process to meet the scaffold function. Some studies focus on full tissue scaffolds, where full protein structure is maintained in hopes of allowing for re-infiltration by stem cells, and subsequent tissue regeneration. Other methods of decellularization utilize enzymes to further break down the protein structures, to fully reduce DNA content from the native tissue. In doing so, broken proteins may for peptide or protein configurations not typically found in the area, particularly for allografted or xenografted decellularized extracellular matrices. In our study, xenografted porcine tissue interacting with murine cells did induce a slight immune response. The decellularized liver, lung and muscle were all digested in pepsin prior to forming the ECM hydrogel construct, and as such were able to control the stiffness of the materials even though the native tissue stiffnesses varied greatly. The broken-down proteins could provide peptides that act as antigens in the MHC II antigen presentation macrophages. When phagocytized along with the remnant DNA and other danger signals, increases in TNFα and IL-1β lead to further macrophage activation as well as lymphocytic activation. T cells would then be activated, and from the MHC II antigen presentation, CD4+ T helper cell proliferation would occur as discovered in the co-culture study for the treatment groups. While inflammatory activation from decellularized matrices is not an entirely novel phenomenon, the influence on the adaptive immune system has not been elucidated,

and further studies will have to be conducted to confirm the mechanism of action for this activation pathway. Since it has been shown to be capable of activating macrophages and influencing the activation of CD4+ T helper cells, then could this activation via antigen presentation lead to further influence in the adaptive immune system and potentially a memory or auto-immune like response to these peptides? In clinical translation, the utilization of decellularized matrices would typically be for a disease-state patient or model. The addition of digested extracellular matrices in an immune-compromised system may lead to further presentation of digested proteins as antigens, leading to an enhanced adaptive immune response. In particular, the presentation of these antigens could lead to a memory or autoimmune-like response, particularly in cases that may require multiple treatments.

Chapter 5 – Aim 2

Decellularized Matrices Effect on the Adaptive Immune Response *In Vivo*

Introduction

From the previous aim we found that digested decellularized matrices did affect the immune response by macrophages, as well as activation of CD4+ T helper cells. With the proteins broken down to peptides, phagocytotic cells can engulf these peptides and present them as an antigen. This phenomena is more likely to occur if the likelihood of being recognized as self vs. non-self is increased, such as for xenografts. *The objective of this aim is to determine if the decellularized matrix constructs influence the adaptive immune response in vivo, and if repeated treatments lead to a lengthened and elevated immune response*. When the adaptive immune response binds to antigens, they can then begin recruiting other cells such as B cells to replicate and produce antibodies for this antigen. In addition, B cells that contain the antibody can remain dormant as a memory cell, such that when activated by the specified antigen, they begin producing antibodies initializing the pro-inflammatory feedback loop. *We hypothesize that digested decellularized extracellular matrix constructs induce a pro-inflammatory response in vivo, and shift the adaptive immune response toward pro-inflammatory CD4+ subsets Th1 and Th17. In addition, repeated treatments of these constructs will further initialize and lengthen the pro-inflammatory response.*

Materials and Methods

Animals and Surgical Procedure

For each study, 8 to 12-week female C57Bl/6 mice (The Jackson Laboratory, Bar Harbor, ME) were used. Animal handling procedures were performed under the approval of the Virginia Commonwealth University Institutional Animal Care and Use Committee (Protocol: AD10001108). Surgeries were performed between 8am and 12pm with mice randomly assigned to groups. 100 microliters of hydrogel sample were injected into the right femoral medullary canal of mice via a medial parapatellar arthrotomy as previously described [43]. Prior to procedures, mice were anesthetized by inhalation of 5% isoflurane gas in O2 and weighed (weight range 19-22g). Legs were prepared by shaving and cleaned with isopropanol and chlorhexidine. Mice were maintained under anesthesia by isoflurane gas to effect during preparation and surgical procedures. To place the hydrogel implant an 8 mm incision was made with a scalpel over the distal side of the knee. The knee ligaments and patella were then moved aside to expose the intercondylar notch of the femur. A 1 mm round dental burr was used to penetrate into the bone and access the medullary canal. Extracellular matrix hydrogel samples were then injected into the medullary canal. Three successful implants were performed for each hydrogel type. After implant placement, periosteal tissue was replaced and closed using resorbable sutures and surgical incisions closed with wound clips. Animals were treated with 0.01mg/kg buprenorphine SR LAB prior to recovery from anesthesia to relieve post-operative pain. Animals were monitored until initial ambulation and every 24 hours for the first 3 days following surgery. Secondary surgery animal groups were treated under the same protocol as previously mentioned following

21 days after initial surgery. For secondary treatment groups and the 14 day post surgery groups the staples were removed following 7 days post treatment. All animals were single housed following surgical procedure, with standard 12-hour light dark cycle and access to food and water ad libitum for the duration of the study. No signs of infection were present in this study.

Flow Cytometry Analysis

Changes in local cell populations were quantified by flow cytometry of bone marrow cells after 3, 7 or 14 days. Systemic changes were measured lymph nodes and spleens. Prior to staining, Fc receptors were blocked by incubation with CD16/32 (BioLegend, San Diego, CA) and membranes permeabilized for transcription factor staining. Macrophage populations were measured in the bone marrow as well as liver with M1 and M2 positive antibody stainings [CD11b – FITC, CD86 (M1) – PE, CD206 (M2) – APC].The ratio of b-cell and t-cell population was determined in lymph and spleens (T cell: PE-CD3, B cell: APC-CD29) (Biolegend). T cell populations were compared in lymph nodes, spleen and bone marrow (PE-CD3, APC-CD4, FITC-CD8). In addition T cell populations in the spleen and lymph nodes were identified by antibodies against T-helper cell marker CD4 (APC-CD4, Biolegend), as well as transcription factors of specific T cell populations [Th1 (PE-Tbet), Th2 (Alexa 488-Gata3), Th17 (PE-RORγT, BD Biosciences), and Treg (Alexa 488-Foxp3)] (Biolegend). Cells were fixed and permeabalized for intracellular staining using Foxp3 Transcription Factor Staining Kit (eBiosciences, Thermofisher). Antibody concentrations were added based on manufacturer's protocol. Stained cell suspensions were analyzed using the Guava® easyCyte 6-2L Benchtop Flow Cytometer (MilliporeSigma) instrument with a

total of 10,000 events were measured with three replicates for each measurement. Results were analyzed using guava Soft 3.1.1 InCyte software.

Circulating Inflammation

Serum was isolated from circulating blood collected 3, 7 and 14 days post material implantation by cardiac puncture. Following Cytokine levels were quantified by Enzyme-Linked immunoSorbant Assays (ELISAs) for pro-inflammatory (IL-6, TNF, IL-1B, IL-17) and anti-inflammatory (IL-10) factors. Cytokine levels were analyzed and normalized to protein per mL serum based off of the dilutions applied to collected whole blood. Standard curves of the serial dilutions provided the method to quantify the amplification when reading at 450 nm.

Statistical Analysis

A one-factor, equal-variance analysis of variance (ANOVA) was used totest the null hypothesis that the group means are equal, against an alternative hypothesis that at least two of the group means are different, at the $\alpha=0.05$ significance level. Upon determination of a p-value less than 0.05 from the overall ANOVA model, multiple comparisons between the group means were made using the Tukey-HSD method. All statistical analysis was completed using GraphPad V5 software.

Results and Discussion

In Vivo Local Macrophage Activation

To assess the effect of the decellularized extracellular matrix constructs on the local inflammatory microenvironment, macrophage activation was measured in the bone marrow at the site of hydrogel injection. In our first study, GelMA, liver, lung and muscle hydrogels were injected into the medullary cavity in one standard surgery. At three days post-surgery surface markers for inflammatory macrophages (CD86+) were significantly elevated in each treatment group in comparison to the GelMA and control groups, with liver and muscle both increasing the highest (Figure 5). The GelMA group saw no statistical difference in pro-inflammatory surface markers in comparison to the control. By 7 days, CD86+ cells were still significantly elevated in the decellularized matrix groups in comparison to the control and GelMA groups, though the percentage of inflammatory macrophages were attenuated in each case. Anti-inflammatory (CD206+) macrophages were elevated in each of the treatment groups including GelMA in comparison to the control 3 days following surgery. By 7 days, anti-inflammatory macrophages were still elevated, and have increased in comparison to the 3 day counterpart . This would be as expected, where the macrophage polarization shifts over time at the injury site from inflammatory (M1) to anti-inflammatory (M2) as the healing process commences.

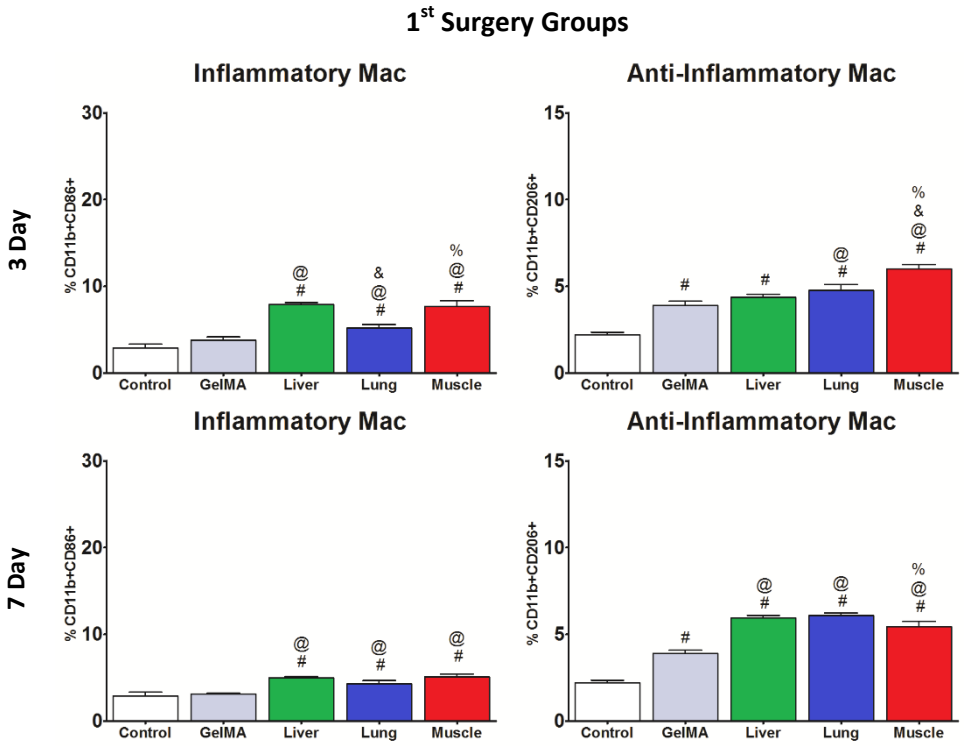

Figure 5: Local changes in macrophage phenotype populations in the bone marrow between single surgery treatment groups (n=3) at 3 and 7 days post-surgery. Inflammatory macrophages (M1) denoted by CD11b+ and CD86+ selection while Anti-inflammatory macrophages denoted by CD11b+ and CD206+ selection. # $p<0.05$ vs control, @ vs. GelMA treatment, & vs. Liver treatment, % vs. Lung treatment.

In our second study, GelMA, liver, lung and muscle hydrogels were injected into the medullary cavity over two separate surgery procedures. Following the first surgery, the animal models were allowed to heal for 21 days post treatment, before undergoing the secondary surgery. This methodology helps highlight the memory response of the adaptive immune system. Surface markers for inflammatory and anti-inflammatory macrophages were quantified at 3, 7 and 14 days post secondary surgery to monitor the inflammatory reaction. At 3 and 7 days post secondary surgery, as seen in the single

surgery treatment groups, the inflammatory macrophage phenotype was significantly increased in comparison to the GelMA and control group counterparts (Figure 6). In contrast, the GelMA groups showed significantly increased presence of inflammatory macrophages at 3 and 7 days post secondary surgery in comparison to the control, indicating that there is some inflammation associated with being a secondary surgery in comparison to the single surgery groups. At 14 days post-surgery, the difference between the GelMA and control group has been reduced to be no longer statistically significant, which would suggest that by 14 days post secondary surgery the inflammation has been resolved; however, the three extracellular matrix groups while reduced still maintain a significantly elevated level of M1 activation in comparison to the GelMA and control groups. This seems to suggest that while the inflammation may have been resolved following the first surgery after 21 days, the re-introduction of the decellularized matrices influenced the immune system to remain in a longer inflammatory state, presumably due to adaptive immunity.

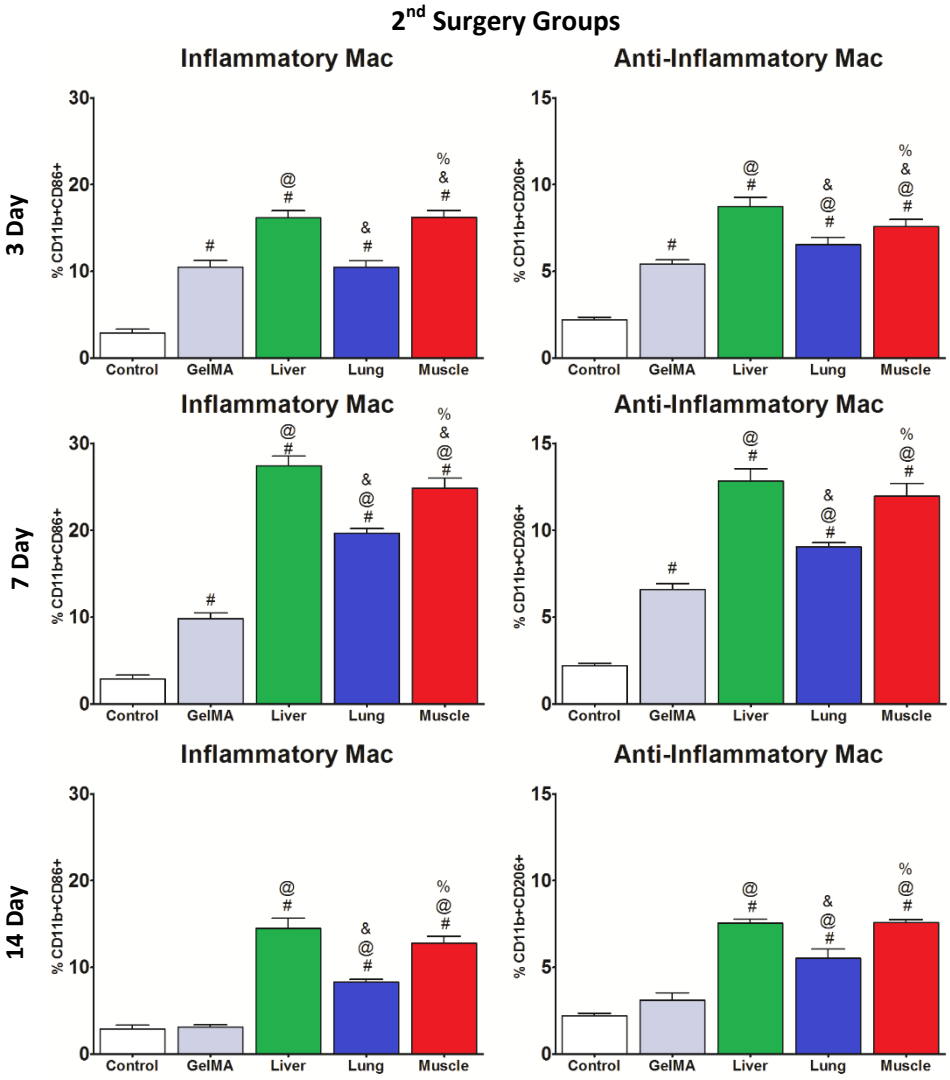

Figure 6: Local changes in macrophage phenotype populations in the bone marrow between secondary surgery treatment groups (n=3) at 3, 7 and 14 days post-surgery. Inflammatory macrophages (M1) denoted by CD11b+ and CD86+ selection while Anti-inflammatory macrophages denoted by CD11b+ and CD206+ selection. # $p<0.05$ vs control, @ vs. GelMA treatment, & vs. Liver treatment, % vs. Lung treatment.

In Vivo Cytokine Secretion

In addition to macrophage activation, systemic inflammatory profile can be quantified by measure of cytokine levels found in whole blood. Pro-inflammatory (IL-1β, IL-6, TNFα and IL-17) cytokines and anti-inflammatory (IL-10) cytokine levels were measured through Enzyme-Linked Immunosorbant Assays, and normalized to a standard provided. In single surgery groups, decellularized matrix treatment groups had significantly elevated levels of all pro-inflammatory cytokines at 3 and 7 days post surgery (Figure 7). From 3 to 7 days, these inflammatory cytokine levels are reduced, suggesting that by 7 days inflammation has run its course, and a more naiive state of inflammation is in place. In the secondary surgery groups, we see extremely elevated levels of pro-inflammatory response at 3 days post surgery. Pro-inflammatory cytokine production of IL-1β, IL-6, TNFα and IL-17 all continue to rise through 7 days post surgery, and begin to attenuate by 14 days post surgery (Figure 8). This suggests a highly elevated as well as lengthened inflammatory response in the secondary surgery groups due to recognition of antigens. This leads to increased Th17 expression and enhanced IL-17 cytokine production.

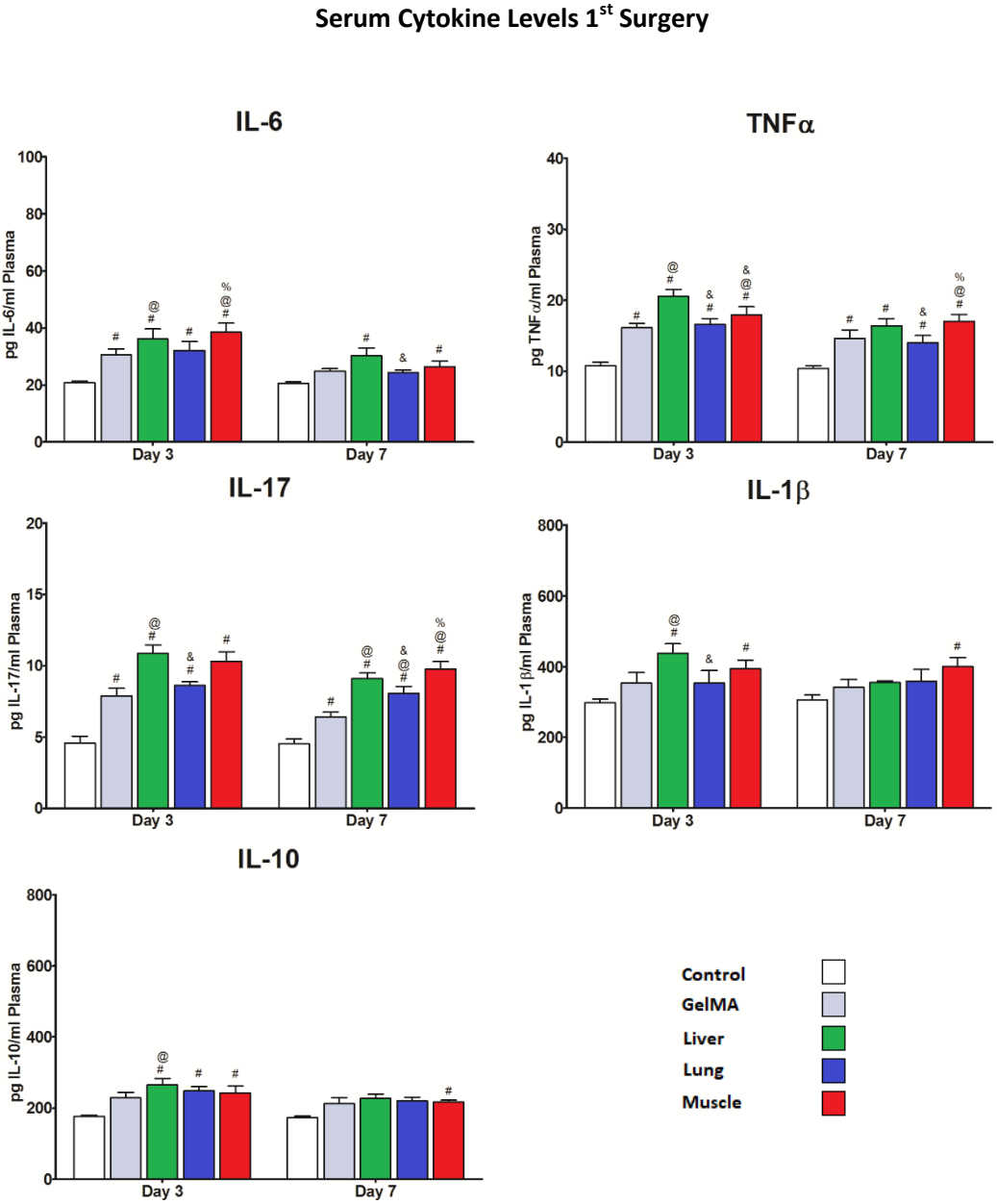

Figure 7: Changes in systemic cytokine levels in circulating plasma for single surgery groups at 3 and 7 days post-surgery (n=3). # $p<0.05$ vs control, @ vs. GelMA treatment, & vs. Liver treatment, % vs. Lung treatment.

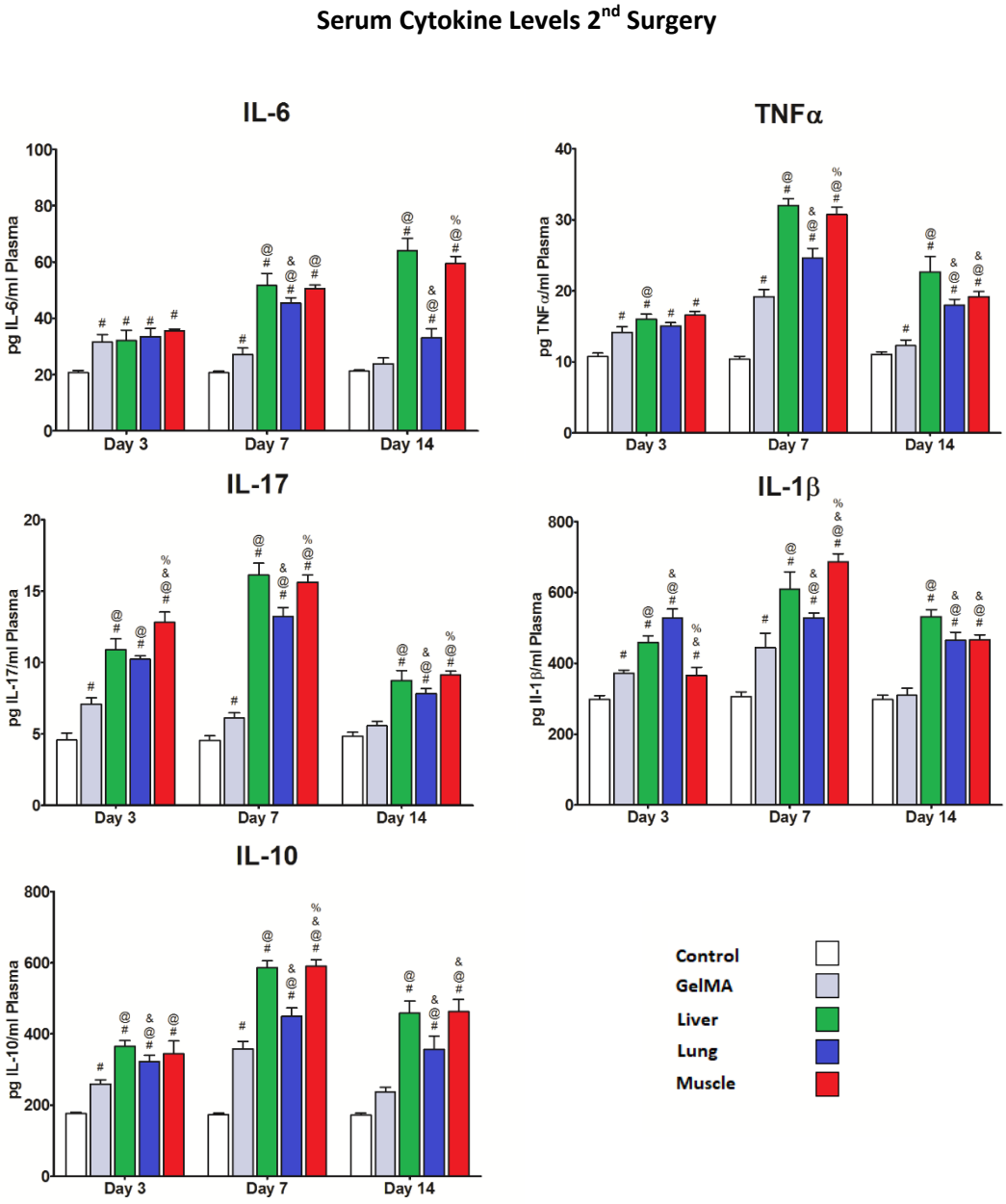

Figure 8: Changes in systemic cytokine levels in circulating plasma for secondary surgery groups at 3 and 7 days post-surgery (n=3). # $p<0.05$ vs control, @ vs. GelMA treatment, & vs. Liver treatment, % vs. Lung treatment.

Local T cell activation

To measure the influence of the extracellular matrix treatments on the local adaptive immune system response, T cell populations were quantified in the bone marrow 3 and 7 days after our primary surgery group. 3 days following the primary surgery, both CD4+ T helper cells and CD8+ Cytotoxic T cells were elevated in decellularized matrix treatment and GelMA treatment in comparison to the control (Figure 9). By 7 days post treatment, CD4+ cells in GelMA treatment groups were no longer significantly elevated in comparison to the control groups. The three decellularized matrix groups all maintained significantly elevated T helper cell incidence at 7 days post surgery compared to the GelMA and control group suggesting that there is an elevated presence of MHC II antigen presentation in the area activating and proliferating CD4+ T cells.

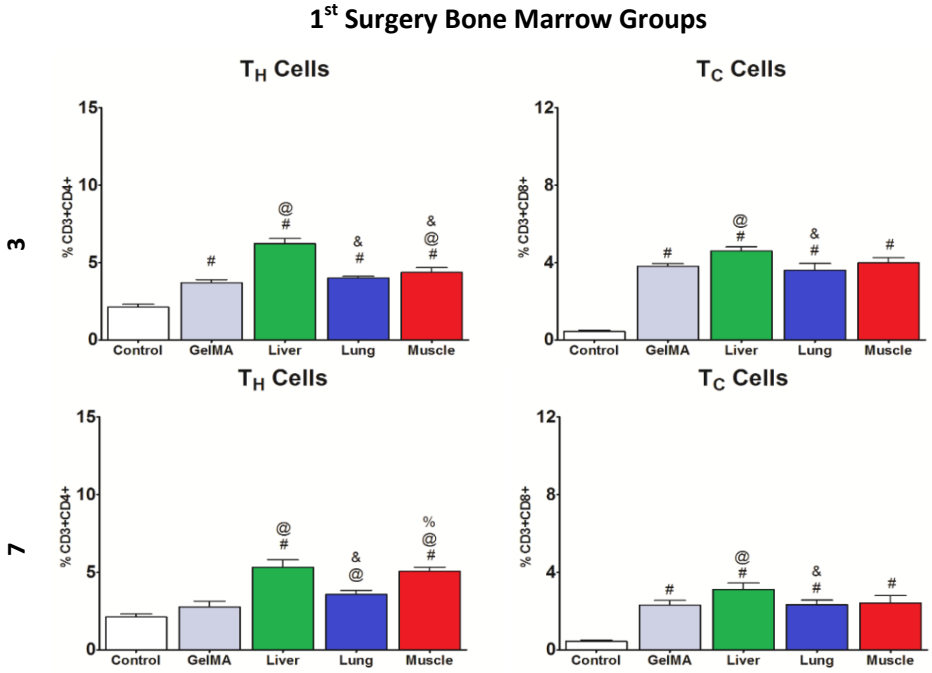

Figure 9: Local changes in T cell populations in the bone marrow between single surgery treatment groups (n=3) at 3 and 7 days post-surgery. T_h signifies T helper cell groups (CD4+) while T_c signifies cytotoxic T cell (CD8+) groups. # $p<0.05$ vs control, @ vs. GelMA treatment, & vs. Liver treatment, % vs. Lung treatment.

In our secondary surgery groups, similar trends are followed as in the primary surgery study. At 3 and 7 days post surgery, decellularized matrix groups have severely elevated levels of CD4+ T helper cells and CD8+ Cytotoxic T cells (Figure 10). While cytotoxic T cells maintain elevated expression throughout in all groups, this can be an indicator of the pro-inflammatory subset of CD4+ cells being elevated. When activated to the Th1 subset, interferon-γ secretion leads to the proliferation of CD8+ T cells. At 3 days post surgery the GelMA treatment group also is significantly elevated T-helper cells compared to control. This activation is no longer statistically significant by day 7 and 14. All three decellularized matrix treatment groups maintain elevated levels of CD4+ T helper cells at 7 and 14 days post-surgery suggesting a prolonged T helper response due to the peptides or danger signals present in the decellularized matrix, and those antigens being potentially “remembered” by the adaptive immune response. When comparing the percentage of local T cells positive for CD4+ in the bone marrow of the secondary surgery groups to primary surgery groups there is a trend toward increased activation in secondary treatments.

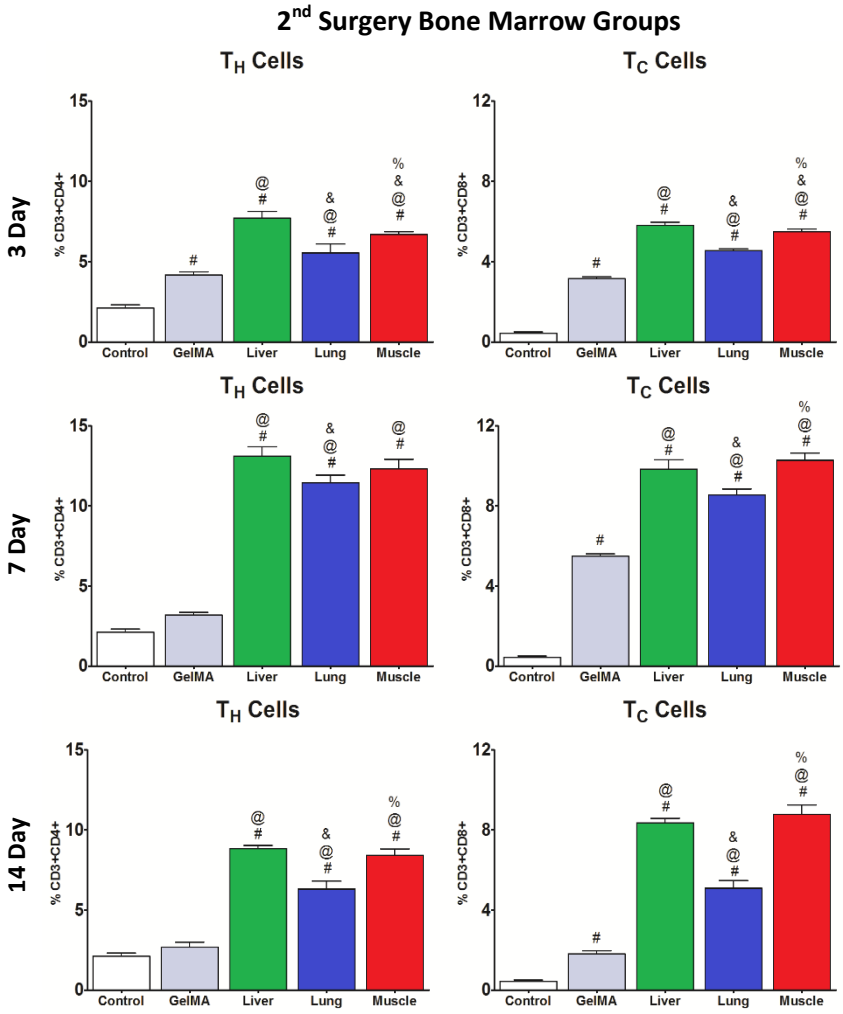

Figure 10: Local changes in T cell populations in the Bone Marrow between treatments in the secondary surgery groups (n=3) at 3, 7 and 14 days post-surgery. T_h signifies T helper cell groups (CD4+) while T_c signifies cytotoxic T cell (CD8+) groups # $p<0.05$ vs control, @ vs. GelMA treatment, & vs. Liver treatment, % vs. Lung treatment.

Local Adaptive Immune Response

To measure the local adaptive immunity, B cells (Figure 13) and CD4+ sub-groups were stained in the right lymph node nearest the surgery site. Similarly to the local response, T cell activation was measured in the right lymph nodes as well. In a

similar trend as previously reported, CD4+ and CD8+ T cell populations were significantly elevated in the decellularized matrix groups in comparison to the GelMA and control groups (Figure 11). These elevated levels were maintained in the lymph node through 3 and 7 days post surgery for single surgery groups. Secondary surgery groups followed a similar trend (Figure 12). At 3 and 7 days post surgery, CD4+ cells were extremely elevated, reaching levels extensively higher than in the primary surgery group. This could be due to communication with antibodies produced by t effector or B cells which constitutes the memory response of the adaptive immunity.

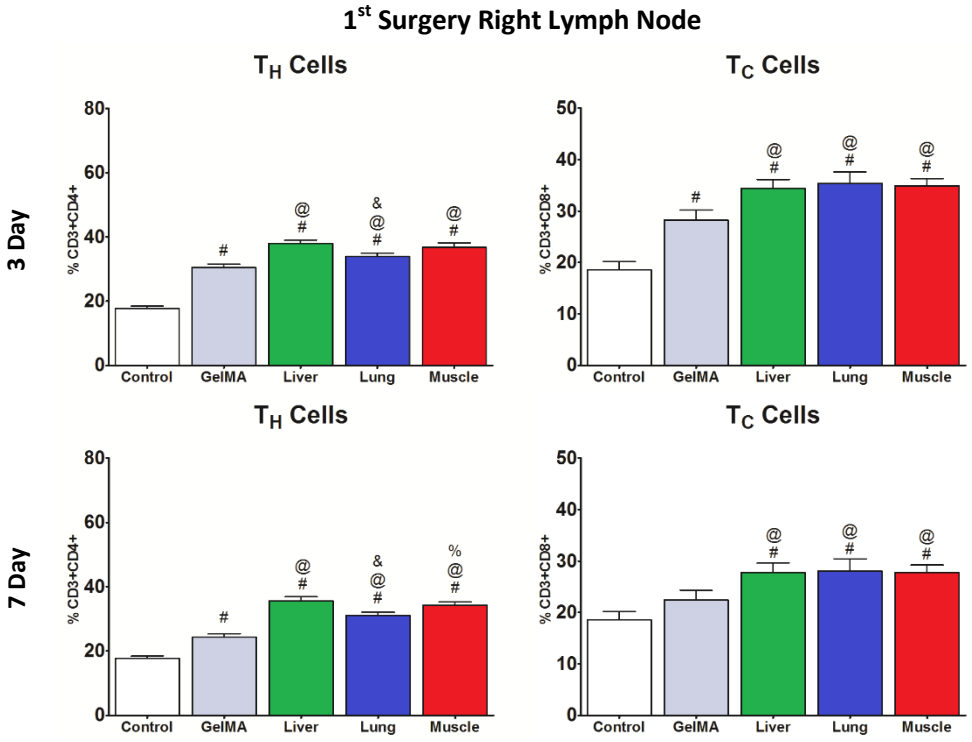

Figure 11: Local changes in T cell populations in the right lymph node between single surgery treatment groups (n=3) at 3 and 7 days post-surgery. T_h signifies T helper cell groups (CD4+) while T_c signifies cytotoxic T cell (CD8+) groups. # $p<0.05$ vs control, @ vs. GelMA treatment, & vs. Liver treatment, % vs. Lung treatment.

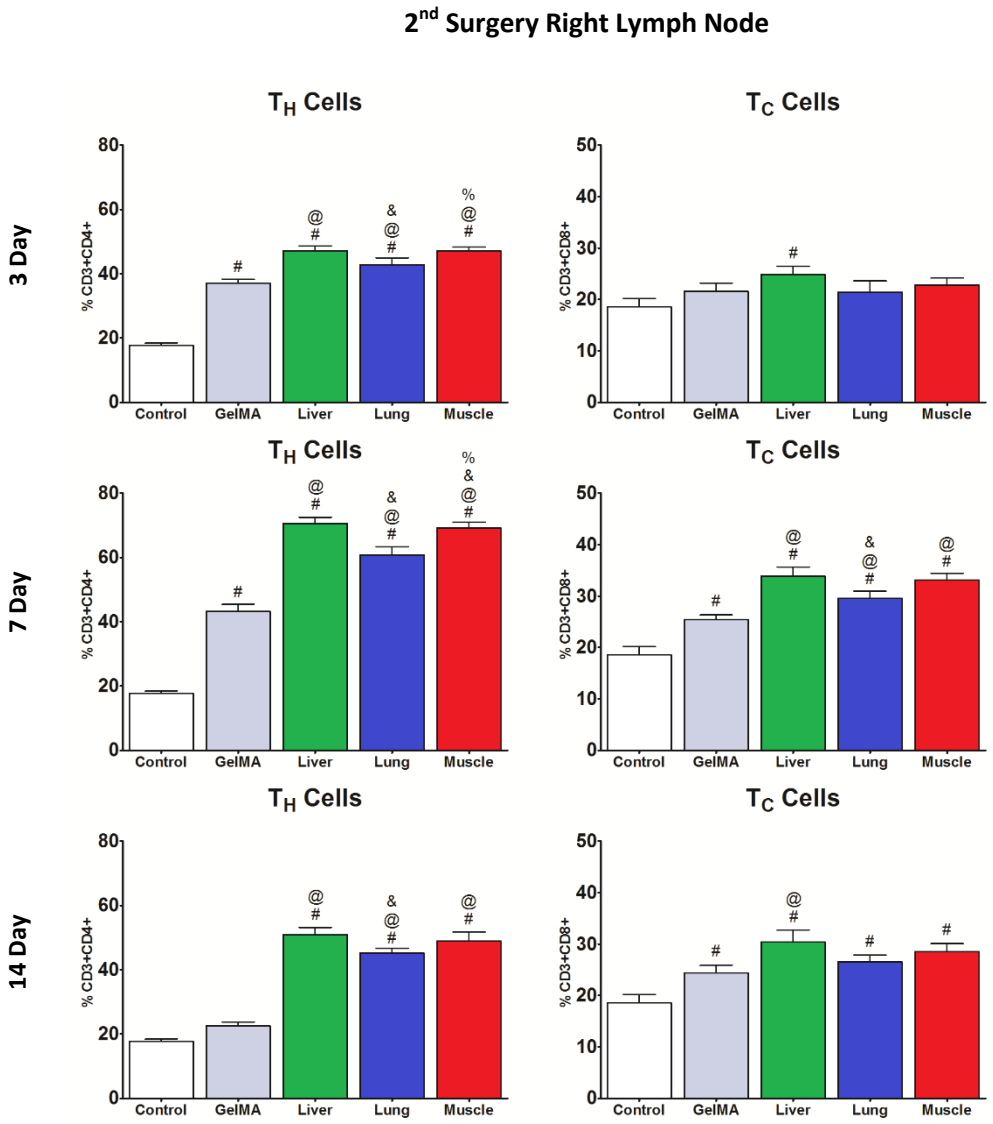

Figure 12: Changes in T cell populations in the right lymph nodes between secondary surgery treatment groups (n=3) at 3, 7 and 14 days post-surgery. T_h signifies T helper cell groups (CD4+) while T_c signifies cytotoxic T cell (CD8+) groups. # $p<0.05$ vs control, @ vs. GelMA treatment, & vs. Liver treatment, % vs. Lung treatment.

To look into more specifically how the T helper cells are influencing the immune response and local microenvironment, T helper cell populations were stained for four primary subsets: Th1, Th2, Th17, and Treg. In the first study consisting of one single surgery, Th1 and Th17, classically considered pro-inflammatory T helper cell subsets see significant increases in activation in all decellularized matrix groups in comparison to the GelMA and control. This is maintained through seven days in all groups, with Th1 levels in the lung treatment group reducing lower levels, though maintain a significant increase compared to the control. This would suggest that the hydrogel constructs, as well as the surgeries themselves would shift the CD4+ T helper cells toward a pro-inflammatory response via Th1 and Th17 activation (Figure 14). Generally this response then seems to shift back toward anti-inflammatory as Treg subpopulations increase dramatically between day 3 and 7 post surgery, and Th17 levels begin to drop off.

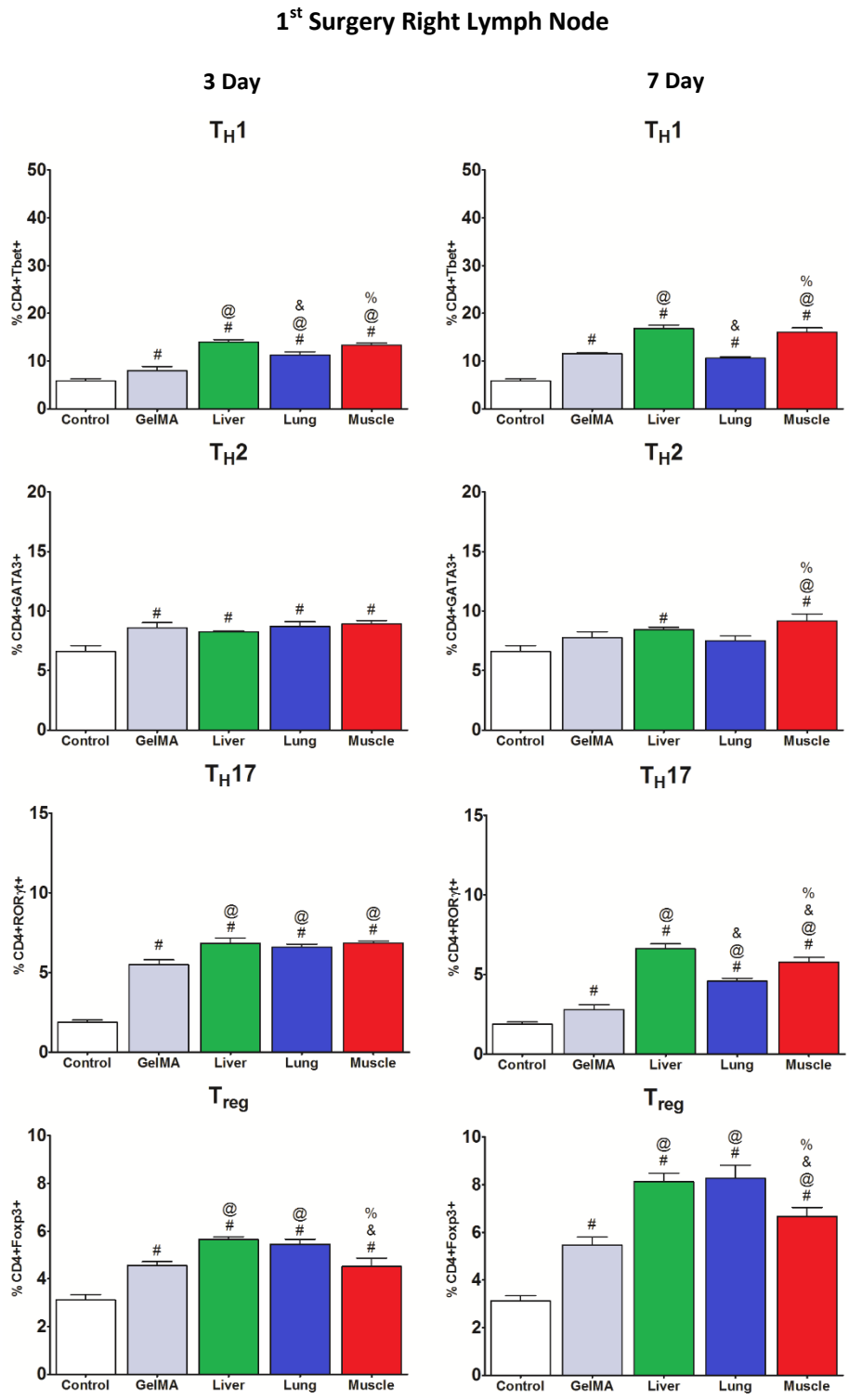

Figure 14: Changes in T helper cell populations in the lymph node between single surgery treatment groups (n=3) at 3 and 7 days post-surgery. Following CD4% selection, transcription factor staining for Tbet (T_H1), Gata3 (T_H2), RORγt (T_H17) and Foxp3 (Treg) identified T helper cell subsets. # $p<0.05$ vs control, @ vs. GelMA treatment, & vs. Liver treatment, % vs. Lung treatment.

In the secondary surgery groups, T helper cell populations follow a similar trend as was discussed previously though delayed. At 3 and 7 day post secondary surgery, pro-inflammatory Th1 and Th17 subsets are increasing dramatically and reaching their peak at 7 days (Figure 15). Previously in single surgery groups, extracellular matrix treatment groups reached their highest increase at day 3, and begin reducing with elevated Treg ctivation at 7 days. For secondary surgery groups, pro-inflammatory T helper cells did not begin attenuating until day 14, at which point Treg activation is increased dramatically. This overall trend suggests that the secondary treatment groups are extending the pro-inflammatory response, and shifting the CD4+ T helper cells primarily toward Th1 and Th17 phenotypes. The Th1 phenotype is the prime driver of the positive inflammatory feedback loop through interferon-γ secretion. Th17 is classically known as a link between adaptive and immune systems, and a driver of the pathogenesis of multiple autoimmune disorders [44], [45]. The increased prevalence of pro-inflammatory Th17 cells also induce the activation and proliferation of B cells (Figure 13). These B cells can then provide antibodies to the antigen or go dormant as memory cells.

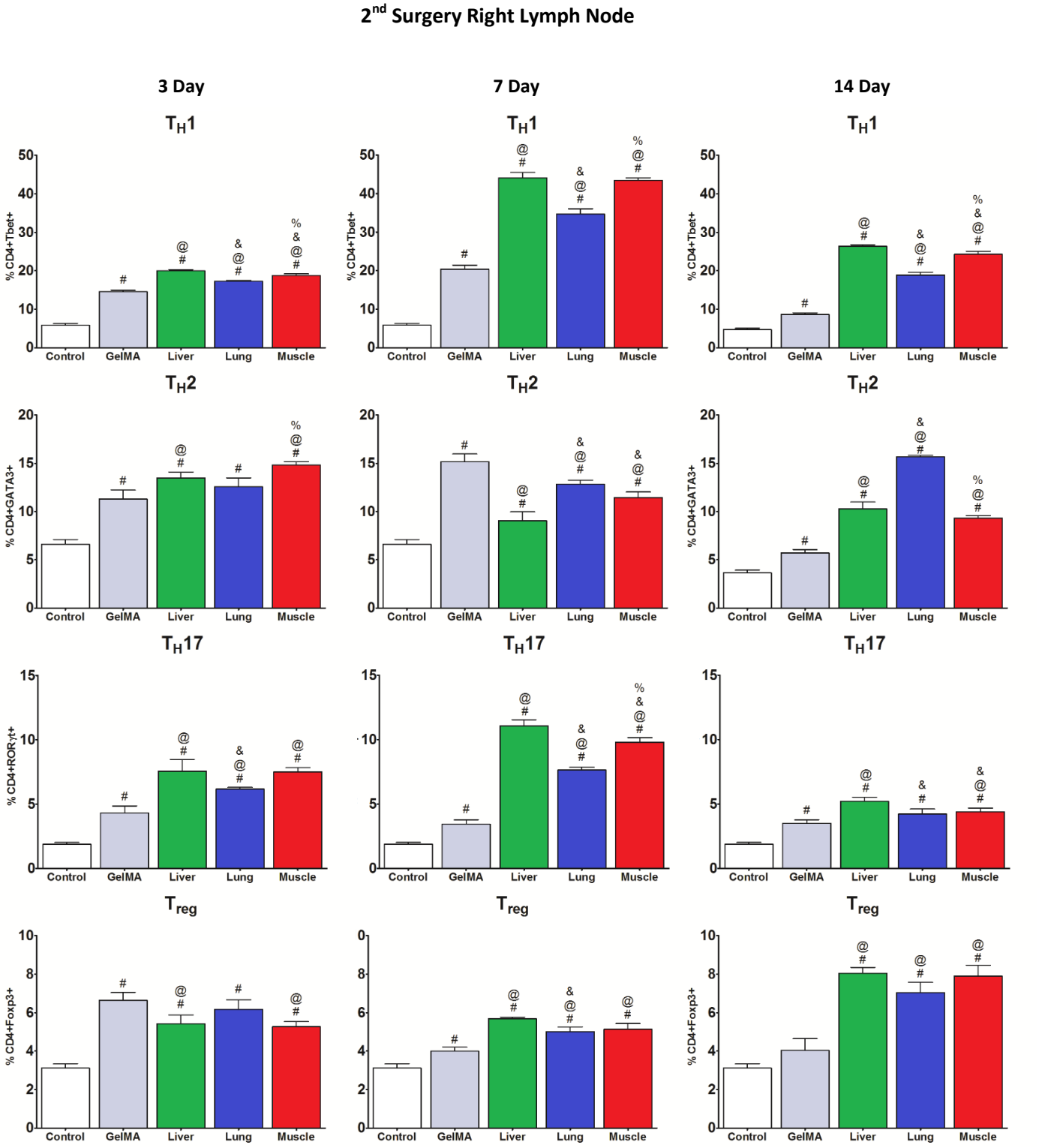

Figure 15: Changes in T helper cell populations in the lymph node between secondary surgery treatment groups (n=3). Following CD4% selection, transcription factor staining for Tbet (T_H1), Gata3 (T_H2), RORγt (T_H17) and Foxp3 (Treg) identified T helper cell subsets. # $p<0.05$ vs control, @ vs. GelMA treatment, & vs. Liver treatment, % vs. Lung treatment.

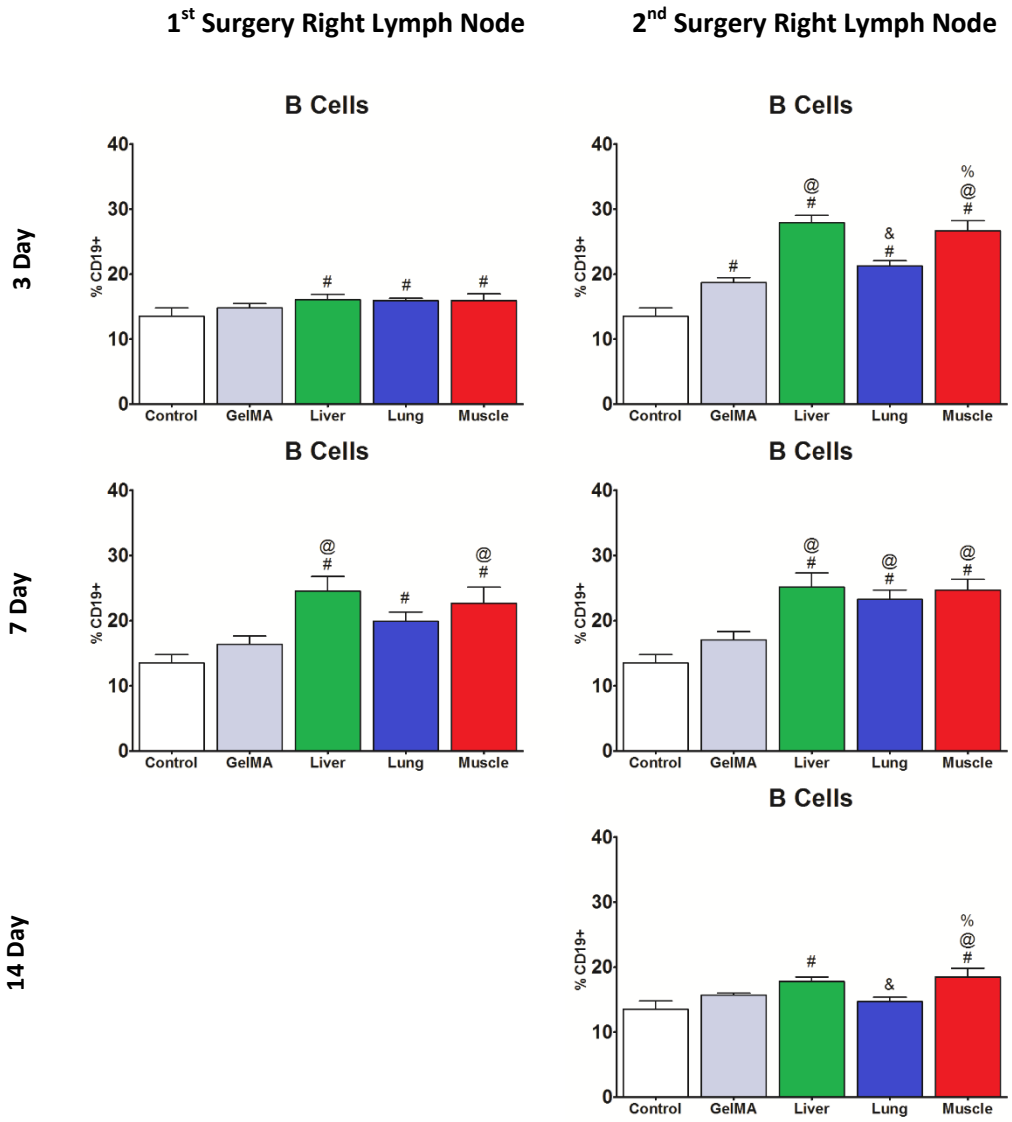

Figure 13: Changes in B cell populations in the right lymph node between single and secondary surgery treatment groups (n=3) at 3, 7 and 14 days post-surgery through CD19+ staining selection. # $p<0.05$ vs control, @ vs. GelMA treatment, & vs. Liver treatment, % vs. Lung treatment.

Systemic Adaptive Immune Response

In addition, similar studies were conducted in the spleen to measure the systemic adaptive immune response. All treatment groups showed elevated levels of CD3+ T cells in the spleen in both single and secondary surgery groups. The number of T cells then increases over time, with increases from 3 to seven days in each surgery group. This increase is not seen with the GelMA treatment, further solidifying the proteins in the decellularized matrix as the driving force of the T cell activation. In the same trend as seen int the pervious study, CD4+ and CD8+ T cell populations were significantly elevated in the decellularized matrix groups in comparison to the GelMA and control groups at 3 and 7 days post-surgery for single surgery groups (Figure 16). Secondary surgery groups see greater increases in T helper cells comparatively, and while reduced the T helper cell activation is maintained through 14 days post secondary surgery in the decellularized matrix treatments (Figure 17).

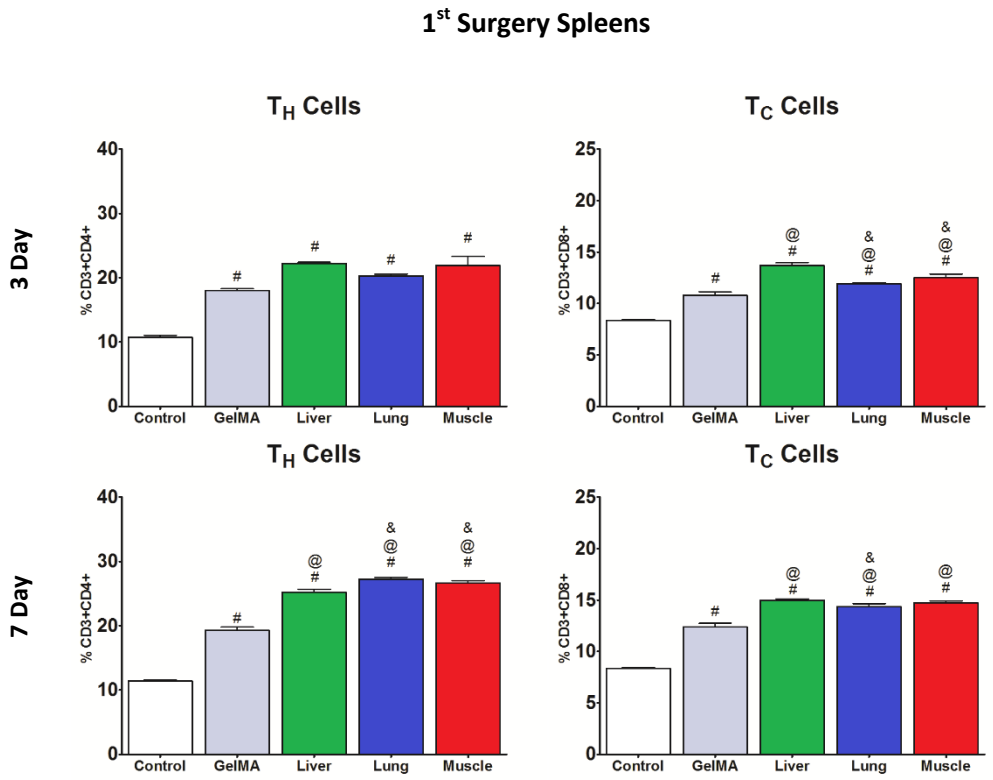

Figure 16: Changes in T cell populations in the spleen between single surgery treatment groups (n=3) at 3 and 7 days post-surgery. T_h signifies T helper cell groups (CD4+) while T_c signifies cytotoxic T cell (CD8+) groups. # $p<0.05$ vs control, @ vs. GelMA treatment, & vs. Liver treatment, % vs. Lung treatment.

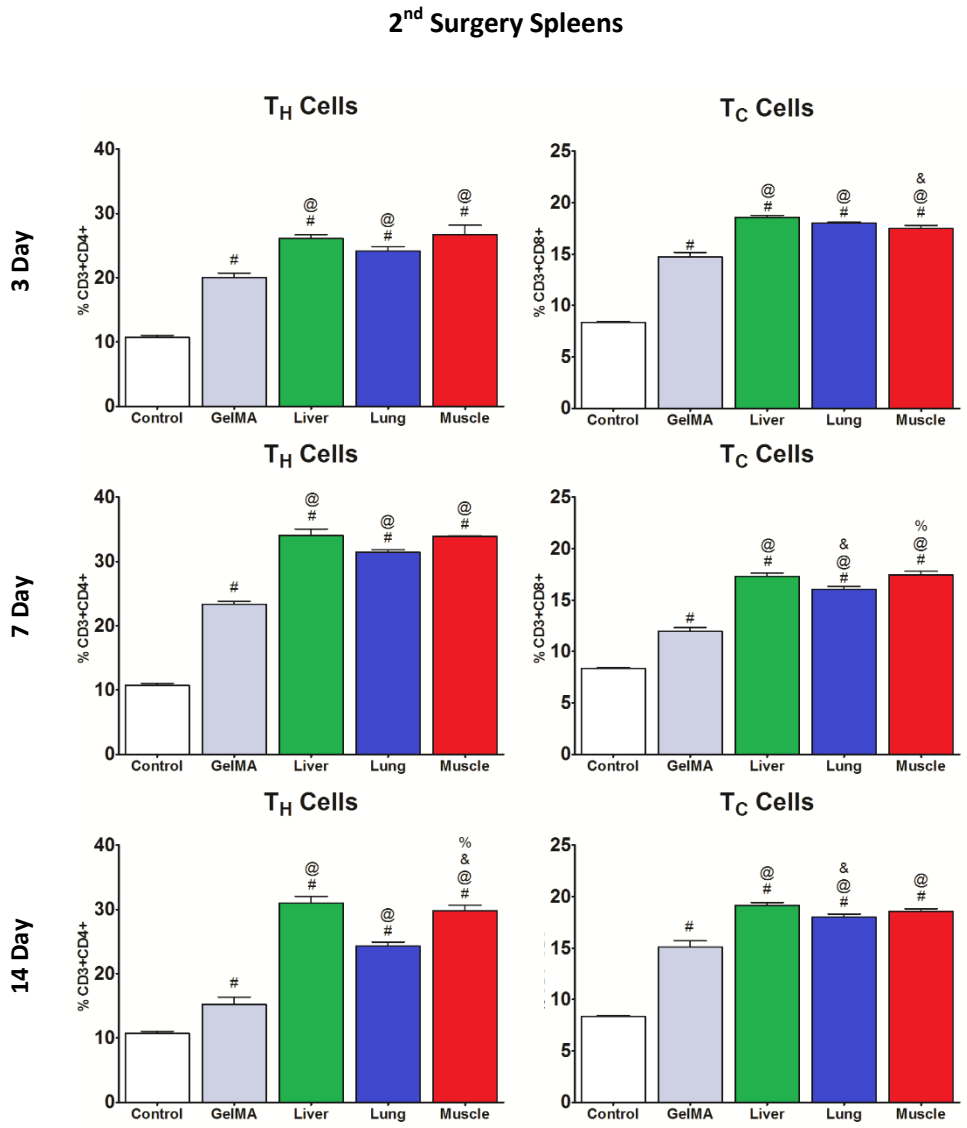

Figure 17: Changes in T cell populations in the spleen between secondary surgery treatment groups (n=3) at 3, 7 and 14 days post-surgery. T_h signifies T helper cell groups (CD4+) while T_c signifies cytotoxic T cell (CD8+) groups. # $p<0.05$ vs control, @ vs. GelMA treatment, & vs. Liver treatment, % vs. Lung treatment.

Systemically, there is a slight shift in the populations in the subsets of the T helper cells. In the lymph node, the Th17 cell populations begin to reduce by 7 days post initial surgery, however systemically these levels are maintained or even further elevated in the 7 day time point in all treatment groups (Figure 18). This can be attributed to the delay in communication of adaptive immune cells and recruitment from the spleen. In the secondary surgery groups, Th17 increases rapidly from day 3 post surgery to day 7 post surgery before reducing as the phenotype shifts toward Th2 at 14 days (Figure 19).

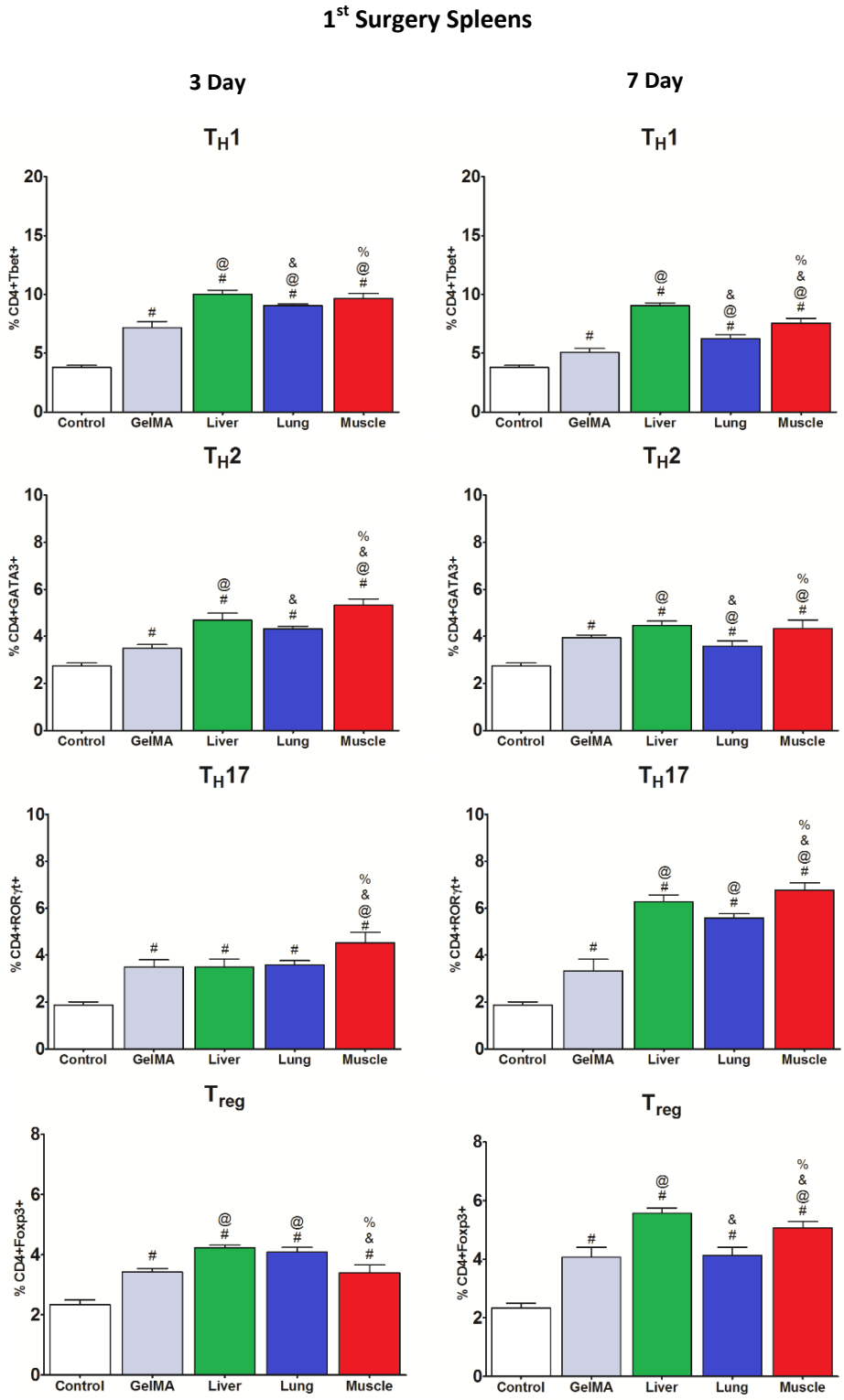

Figure 18: Changes in T helper cell populations in the spleen between single surgery treatment groups (n=3) at 3 and 7 days post-surgery. Following CD4% selection, transcription factor staining for Tbet (T_H1), Gata3 (T_H2), RORγt (T_H17) and Foxp3 (Treg) identified T helper cell subsets. # $p<0.05$ vs control, @ vs. GelMA treatment, & vs. Liver treatment, % vs. Lung treatment.

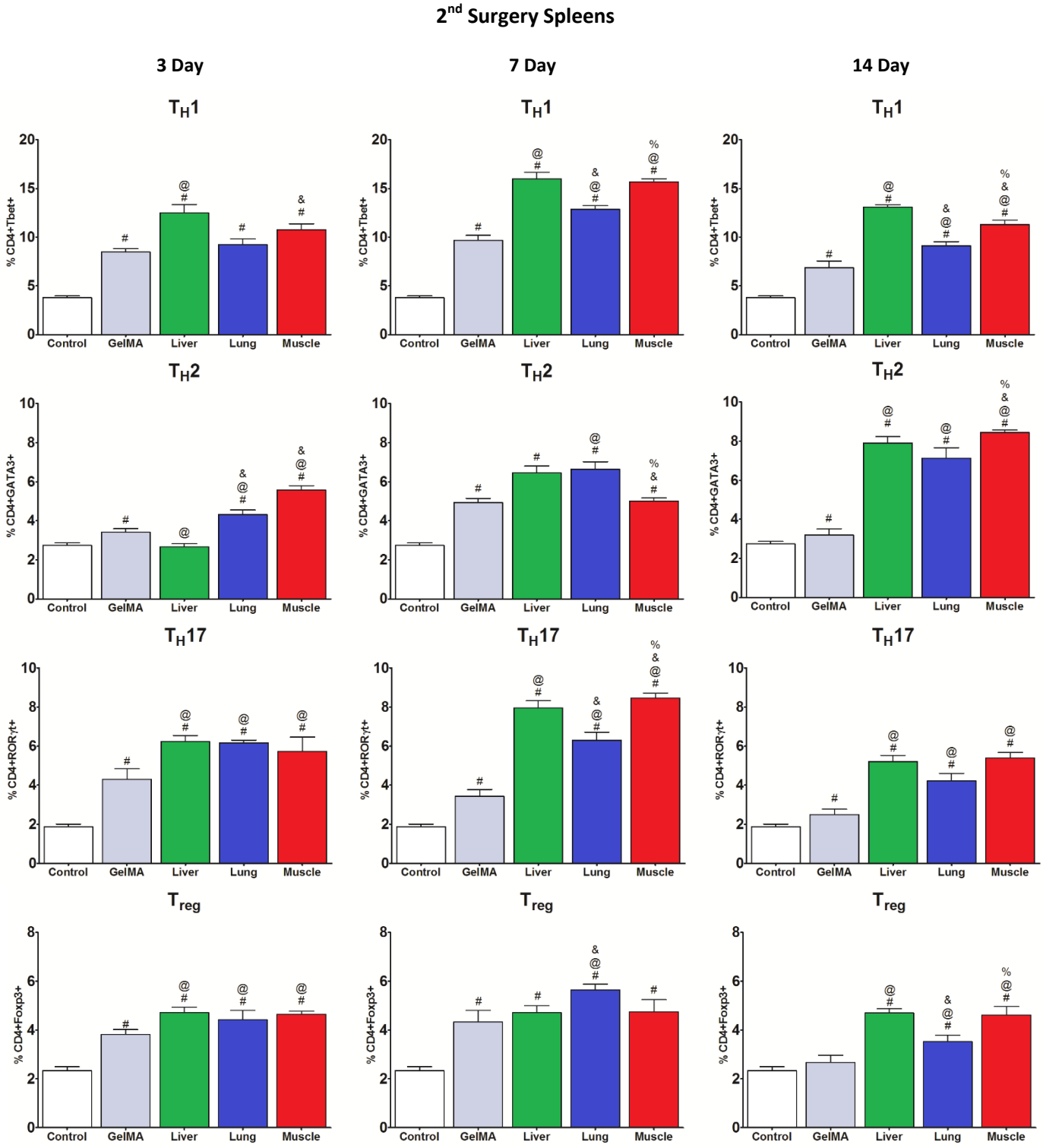

Figure 19: Changes in T helper cell populations in the spleen between secondary surgery treatment groups (n=3). Following CD4% selection, transcription factor staining for Tbet (T_H1), Gata3 (T_H2), RORγt (T_H17) and Foxp3 (Treg) identified T helper cell subsets. # $p<0.05$ vs control, @ vs. GelMA treatment, & vs. Liver treatment, % vs. Lung

Conclusion

In vitro analysis showed the potential of antigen presentation of digested proteins from decellularized matrices in the activation of CD4+ T helper cells and subsequent proliferation. When applied to the *in vivo* setting through medullary cavity injection, decellularized extracellular matrices produced an inflammatory reaction toward the M1 macrophage phenotype, that was mostly resolved over 7 days denoted by increases in M2 macrophage phenotypes. When the animals were subjected to secondary surgeries three weeks following their initial surgery, the inflammatory profile was increased, and seemed to linger beyond the 7 day mark. While this could be attributed solely to the second surgery itself, GelMA groups without decellularized matrices additives showed attenuation of this inflammatory response, with M1 phenotype macrophages reducing to near control levels in the bone marrow. The decellularized matrix treatment groups showed a sustained M1 macrophage phenotype in the bone marrow cavity persisting for 14+ days following secondary surgery. This increase in sustained inflammation may be due to a memory response from the adaptive immune system as similar peptides and danger signals activate the CD4+ T helper cell response.

This trend was followed when T cell populations were identified in the bone marrow as well as local lymph node. Secondary surgery groups showed persistent elevated levels of CD4+ T helper cells in the bone marrow in comparison to the single surgery groups. Right lymph node CD4+ T helper cell populations also showed increases in the secondary surgery group in comparison to the primary surgery group, as would be expected. Interestingly, CD8+ cytotoxic T cells showed elevated levels in the secondary surgery groups when compared with the single surgery groups. This

would not be expected, as CD8+ Cytotoxic T cells are generally activated by MHC I antigen presentation, however Th1 subsets of CD4+ T cells produce interferon-γ which stimulates the CD8+ activation in a positive feedback loop. The secondary surgery groups showed elevated levels of Th1 populations in both the local (lymph node) as well as systemic (spleen) CD4+ populations. In addition to elevated Th1 populations, the secondary surgery groups had elevated levels of Th17 populations which greatly influence the adaptive immune response. Th17 cells are one of the primary modulators in autoimmunity, and increases in Th17 activity as well as IL-17 production denote an extremely pro-inflammatory setting buoyed by antigen memory in CD4+ activation. When subjected to multiple treatments of decellularized extracellular constructs, the lengthened and heightened inflammatory response mediated by elevated Th1 and Th17 levels indicates that the repeated treatments of digested extracellular matrices provided the antigens to influence the adaptive immune response, and provide a short-term memory response. Overall, this suggests that when choosing the methodologies of processing of decellularized matrices, further testing is needed to ensure that the adaptive immune response to broken down peptides is minimized.

List of References

[1] S. F. Badylak, “The extracellular matrix as a biologic scaffold material,” *Biomaterials*, vol. 28, no. 25, pp. 3587–3593, Sep. 2007.

[2] P. K. Vallittu, B. H. Durgesh, A. A. AlKheraif, and J. Hjerppe, “From body-on-frame to unibody constructions and designs mimicking biological structures - an overview,” *Eur. J. Oral Sci.*, vol. 126, pp. 95–101, Oct. 2018.

[3] K. M. Hotchkiss, G. B. Reddy, S. L. Hyzy, Z. Schwartz, B. D. Boyan, and R. Olivares-Navarrete, “Titanium surface characteristics, including topography and wettability, alter macrophage activation,” *Acta Biomater.*, vol. 31, pp. 425–434, Feb. 2016.

[4] G. Cervino *et al.*, “Fem and Von Mises Analysis of OSSTEM Dental Implant Structural Components: Evaluation of Different Direction Dynamic Loads,” *Open Dent. J.*, vol. 12, no. 1, pp. 219–229, Mar. 2018.

[5] I. Linetskiy, V. Demenko, L. Linetska, and O. Yefremov, “Impact of annual bone loss and different bone quality on dental implant success – A finite element study,” *Comput. Biol. Med.*, vol. 91, pp. 318–325, Dec. 2017.

[6] S. Zhang *et al.*, “Thermoresponsive Copolypeptide Hydrogel Vehicles for Central Nervous System Cell Delivery,” *ACS Biomater. Sci. Eng.*, vol. 1, no. 8, pp. 705–717, Aug. 2015.

[7] K. Sternberg *et al.*, “Implant-associated local drug delivery systems based on biodegradable polymers: customized designs for different medical applications,” *Biomed. Tech. Eng.*, vol. 58, no. 5, Jan. 2013.

[8] J. S. Auerbach and C. K. Schott, “Solid-Organ Graft-Versus-Host Disease After Liver Transplant: A Case Report,” *Crit. Care Nurse*, vol. 36, no. 3, pp. e7–e11, Jun. 2016.

[9] A. Pacifici *et al.*, “Decellularized Hydrogels in Bone Tissue Engineering: A Topical Review,” *Int. J. Med. Sci.*, vol. 15, no. 5, pp. 492–497, 2018.

[10] D. A. Taylor, L. C. Sampaio, Z. Ferdous, A. S. Gobin, and L. J. Taite, “Decellularized matrices in regenerative medicine,” *Acta Biomater.*, vol. 74, pp. 74–89, Jul. 2018.

[11] M. Misfeld and M. A. Borger, “The Ross procedure: Time to reevaluate the guidelines,” *J. Thorac. Cardiovasc. Surg.*, Jul. 2018.

[12] D. Bracey *et al.*, “A Decellularized Porcine Xenograft-Derived Bone Scaffold for Clinical Use as a Bone Graft Substitute: A Critical Evaluation of Processing and Structure,” *J. Funct. Biomater.*, vol. 9, no. 3, p. 45, Jul. 2018.

[13] S. T. Boyce and A. L. Lalley, “Tissue engineering of skin and regenerative medicine for wound care,” *Burns Trauma*, vol. 6, no. 1, Dec. 2018.

[14] C. Philips, F. Campos, A. Roosens, M. del C. Sánchez-Quevedo, H. Declercq, and V. Carriel, “Qualitative and Quantitative Evaluation of a Novel Detergent-Based Method for Decellularization of Peripheral Nerves,” *Ann. Biomed. Eng.*, Jul. 2018.

[15] Y. Seo, Y. Jung, and S. H. Kim, “Decellularized heart ECM hydrogel using supercritical carbon dioxide for improved angiogenesis,” *Acta Biomater.*, vol. 67, pp. 270–281, Feb. 2018.

[16] S. Rahman, M. Griffin, A. Naik, M. Szarko, and P. E. M. Butler, “Optimising the decellularization of human elastic cartilage with trypsin for future use in ear reconstruction,” *Sci. Rep.*, vol. 8, no. 1, Dec. 2018.
[17] P. A. Link, R. A. Pouliot, N. S. Mikhaiel, B. M. Young, and R. L. Heise, “Tunable Hydrogels from Pulmonary Extracellular Matrix for 3D Cell Culture,” *J. Vis. Exp.*, no. 119, Jan. 2017.
[18] K. M. Hotchkiss, N. M. Clark, and R. Olivares-Navarrete, “Macrophage response to hydrophilic biomaterials regulates MSC recruitment and T-helper cell populations,” *Biomaterials*, vol. 182, pp. 202–215, Nov. 2018.
[19] L. Eckhart and E. Tschachler, “Control of cell death-associated danger signals during cornification prevents autoinflammation of the skin,” *Exp. Dermatol.*, vol. 27, no. 8, pp. 884–891, Aug. 2018.
[20] C. D. M. Robert A Harris, “Macrophage Polarization: Decisions That Affect Health,” *J. Clin. Cell. Immunol.*, vol. 6, no. 5, 2015.
[21] X. Qiu *et al.*, “Mesenchymal stem cells and extracellular matrix scaffold promote muscle regeneration by synergistically regulating macrophage polarization toward the M2 phenotype,” *Stem Cell Res. Ther.*, vol. 9, no. 1, Dec. 2018.
[22] A. H. Morris, J. Chang, and T. R. Kyriakides, “Inadequate Processing of Decellularized Dermal Matrix Reduces Cell Viability *In Vitro* and Increases Apoptosis and Acute Inflammation *In Vivo*,” *BioResearch Open Access*, vol. 5, no. 1, pp. 177–187, May 2016.
[23] S. T. Lopresti and B. N. Brown, “Host Response to Naturally Derived Biomaterials,” in *Host Response to Biomaterials*, Elsevier, 2015, pp. 53–79.
[24] P. W. Dempsey, S. A. Vaidya, and G. Cheng, “The Art of War: Innate and adaptive immune responses,” *Cell. Mol. Life Sci. CMLS*, vol. 60, no. 12, pp. 2604–2621, Dec. 2003.
[25] S. Flaherty and J. M. Reynolds, “Mouse Naiive CD4+ T Cell Isolation and In vitro Differentiation into T Cell Subsets,” *J. Vis. Exp.*, no. 98, Apr. 2015.
[26] L. Jia and C. Wu, “The Biology and Functions of Th22 Cells,” in *T Helper Cell Differentiation and Their Function*, vol. 841, B. Sun, Ed. Dordrecht: Springer Netherlands, 2014, pp. 209–230.
[27] C. Dong and R. A. Flavell, “Cell fate decision: T-helper 1 and 2 subsets in immune responses,” *Arthritis Res.*, vol. 2, no. 3, pp. 179–188, 2000.
[28] A. E. Wakil, Z. E. Wang, J. C. Ryan, D. J. Fowell, and R. M. Locksley, “Interferon gamma derived from CD4(+) T cells is sufficient to mediate T helper cell type 1 development,” *J. Exp. Med.*, vol. 188, no. 9, pp. 1651–1656, Nov. 1998.
[29] S. L. Swain, A. D. Weinberg, M. English, and G. Huston, “IL-4 directs the development of Th2-like helper effectors,” *J. Immunol. Baltim. Md 1950*, vol. 145, no. 11, pp. 3796–3806, Dec. 1990.
[30] L. E. Harrington *et al.*, “Interleukin 17–producing CD4+ effector T cells develop via a lineage distinct from the T helper type 1 and 2 lineages,” *Nat. Immunol.*, vol. 6, no. 11, pp. 1123–1132, Nov. 2005.
[31] H. Liu and C. Rohowsky-Kochan, “Regulation of IL-17 in Human CCR6+ Effector Memory T Cells,” *J. Immunol.*, vol. 180, no. 12, pp. 7948–7957, Jun. 2008.
[32] S. Sakaguchi, T. Yamaguchi, T. Nomura, and M. Ono, “Regulatory T Cells and Immune Tolerance,” *Cell*, vol. 133, no. 5, pp. 775–787, May 2008.

[33] Y. Peng *et al.*, “Alteration of Naïve and Memory B-Cell Subset in Chronic Graft-Versus-Host Disease Patients After Treatment With Mesenchymal Stromal Cells: MSC Treatment Influences B-Cell Homeostasis,” *STEM CELLS Transl. Med.*, vol. 3, no. 9, pp. 1023–1031, Sep. 2014.
[34] D. J. Rawlings, G. Metzler, M. Wray-Dutra, and S. W. Jackson, “Altered B cell signalling in autoimmunity,” *Nat. Rev. Immunol.*, vol. 17, no. 7, pp. 421–436, Apr. 2017.
[35] J. E. Reing *et al.*, “The effects of processing methods upon mechanical and biologic properties of porcine dermal extracellular matrix scaffolds,” *Biomaterials*, vol. 31, no. 33, pp. 8626–8633, Nov. 2010.
[36] B. H. Lee, H. Shirahama, N.-J. Cho, and L. P. Tan, “Efficient and controllable synthesis of highly substituted gelatin methacrylamide for mechanically stiff hydrogels,” *RSC Adv.*, vol. 5, no. 128, pp. 106094–106097, 2015.
[37] D. O. Freytes, J. Martin, S. S. Velankar, A. S. Lee, and S. F. Badylak, “Preparation and rheological characterization of a gel form of the porcine urinary bladder matrix,” *Biomaterials*, vol. 29, no. 11, pp. 1630–1637, Apr. 2008.
[38] M. Nakasaki *et al.*, “The matrix protein Fibulin-5 is at the interface of tissue stiffness and inflammation in fibrosis,” *Nat. Commun.*, vol. 6, no. 1, Dec. 2015.
[39] S. Budday *et al.*, “Mechanical properties of gray and white matter brain tissue by indentation,” *J. Mech. Behav. Biomed. Mater.*, vol. 46, pp. 318–330, Jun. 2015.
[40] F. Y. McWhorter, C. T. Davis, and W. F. Liu, “Physical and mechanical regulation of macrophage phenotype and function,” *Cell. Mol. Life Sci.*, vol. 72, no. 7, pp. 1303–1316, Apr. 2015.
[41] T. W. Gilbert, J. M. Freund, and S. F. Badylak, “Quantification of DNA in Biologic Scaffold Materials,” *J. Surg. Res.*, vol. 152, no. 1, pp. 135–139, Mar. 2009.
[42] M. L. Pinto *et al.*, “Decellularized human colorectal cancer matrices polarize macrophages towards an anti-inflammatory phenotype promoting cancer cell invasion via CCL18,” *Biomaterials*, vol. 124, pp. 211–224, Apr. 2017.
[43] R. Olivares-Navarrete *et al.*, “Osteoblast maturation and new bone formation in response to titanium implant surface features are reduced with age,” *J. Bone Miner. Res.*, vol. 27, no. 8, pp. 1773–1783, Aug. 2012.
[44] M. J. McGeachy, “Th17 memory cells: live long and proliferate,” *J. Leukoc. Biol.*, vol. 94, no. 5, pp. 921–926, Nov. 2013.
[45] L. A. Tesmer, S. K. Lundy, S. Sarkar, and D. A. Fox, “Th17 cells in human disease,” *Immunol. Rev.*, vol. 223, no. 1, pp. 87–113, Jun. 2008.